SECURITY CLASSIFICATION: UNCLASSIFIED

76

COMPONENTS R&D LABORATORIES

LAND LOCOMOTION LABORATORY

Report No. 8091

LL No. 84

Copy No. 104

PERFORMANCE ANALYSIS OF A DRIVEN NON-DEFLECTING TIRE IN SOIL

By

Zoltan J. Janosi

June, 1963

Project No: 5016.11.84400

Authenticated: Ronald A Gibson

D/A Project: 597-01-006

Approved: Stanley Zeller

MOBILITY

U.S. ARMY TANK-AUTOMOTIVE CENTER
CENTER LINE, MICHIGAN

SECURITY CLASSIFICATION: UNCLASSIFIED

"THE FINDINGS IN THIS REPORT ARE NOT TO BE CONSTRUED AS AN OFFICIAL DEPARTMENT OF THE ARMY POSITION"

Unclassified

Security Classification

DOCUMENT CONTROL DATA - R&D

(Security classification of title, body of abstract and indexing annotation must be entered when the overall report is classified)

1. ORIGINATING ACTIVITY (Corporate author)	2a. REPORT SECURITY CLASSIFICATION
Army Tank Automotive Center, Warren, Michigan	Unclassified
	2b. GROUP

3. REPORT TITLE

PERFORMANCE ANALYSIS OF A DRIVEN NON-DEFLECTING TIRE IN SOIL

4. DESCRIPTIVE NOTES (Type of report and inclusive dates)

5. AUTHOR(S) (Last name, first name, initial)

Janosi, Zoltan J.

6. REPORT DATE	7a. TOTAL NO. OF PAGES	7b. NO. OF REFS
June 1963	50 p.	

8a. CONTRACT OR GRANT NO.	9a. ORIGINATOR'S REPORT NUMBER(S)
b. PROJECT NO. 8091	AD 608553
c.	9b. OTHER REPORT NO(S) (Any other numbers that may be assigned this report) LL No. 84
d.	

10. AVAILABILITY/LIMITATION NOTICES

11. SUPPLEMENTARY NOTES	12. SPONSORING MILITARY ACTIVITY

13. ABSTRACT

To analyze the performance of tires in soft soil.

Studies were conducted and an equation relating the drawbar-pull exerted by a wheel operating in soft soil has been derived as a function of slip. It was found that maximum slip is reached at a slippinkage that corresponds to that point of the wheel perimeter that has a vertical instantaneous-velocity vector.

FORM 1 JAN 64 1473

Unclassified

Security Classification

14. KEY WORDS	LINK A		LINK B		LINK C	
	ROLE	WT	ROLE	WT	ROLE	WT
Wheeled vehicle studies Soil mobility studies Tire-in-soil studies Traction versus slip Wheel slippage Tire-soil relationship Soil characteristics						

INSTRUCTIONS

1. ORIGINATING ACTIVITY: Enter the name and address of the contractor, subcontractor, grantee, Department of Defense activity or other organization *(corporate author)* issuing the report.

2*a*. REPORT SECURITY CLASSIFICATION: Enter the overall security classification of the report. Indicate whether "Restricted Data" is included. Marking is to be in accordance with appropriate security regulations.

2*b*. GROUP: Automatic downgrading is specified in DoD Directive 5200.10 and Armed Forces Industrial Manual. Enter the group number. Also, when applicable, show that optional markings have been used for Group 3 and Group 4 as authorized.

3. REPORT TITLE: Enter the complete report title in all capital letters. Titles in all cases should be unclassified. If a meaningful title cannot be selected without classification, show title classification in all capitals in parenthesis immediately following the title.

4. DESCRIPTIVE NOTES: If appropriate, enter the type of report, e.g., interim, progress, summary, annual, or final. Give the inclusive dates when a specific reporting period is covered.

5. AUTHOR(S): Enter the name(s) of author(s) as shown on or in the report. Enter last name, first name, middle initial. If military, show rank and branch of service. The name of the principal author is an absolute minimum requirement.

6. REPORT DATE: Enter the date of the report as day, month, year; or month, year. If more than one date appears on the report, use date of publication.

7*a*. TOTAL NUMBER OF PAGES: The total page count should follow normal pagination procedures, i.e., enter the number of pages containing information.

7*b*. NUMBER OF REFERENCES: Enter the total number of references cited in the report.

8*a*. CONTRACT OR GRANT NUMBER: If appropriate, enter the applicable number of the contract or grant under which the report was written.

8*b*, 8*c*, & 8*d*. PROJECT NUMBER: Enter the appropriate military department identification, such as project number, subproject number, system numbers, task number, etc.

9*a*. ORIGINATOR'S REPORT NUMBER(S): Enter the official report number by which the document will be identified and controlled by the originating activity. This number must be unique to this report.

9*b*. OTHER REPORT NUMBER(S): If the report has been assigned any other report numbers *(either by the originator or by the sponsor)*, also enter this number(s).

10. AVAILABILITY/LIMITATION NOTICES: Enter any limitations on further dissemination of the report, other than those imposed by security classification, using standard statements such as:

(1) "Qualified requesters may obtain copies of this report from DDC."

(2) "Foreign announcement and dissemination of this report by DDC is not authorized."

(3) "U. S. Government agencies may obtain copies of this report directly from DDC. Other qualified DDC users shall request through _____."

(4) "U. S. military agencies may obtain copies of this report directly from DDC. Other qualified users shall request through _____."

(5) "All distribution of this report is controlled. Qualified DDC users shall request through _____."

If the report has been furnished to the Office of Technical Services, Department of Commerce, for sale to the public, indicate this fact and enter the price, if known.

11. SUPPLEMENTARY NOTES: Use for additional explanatory notes.

12. SPONSORING MILITARY ACTIVITY: Enter the name of the departmental project office or laboratory sponsoring *(paying for)* the research and development. Include address.

13. ABSTRACT: Enter an abstract giving a brief and factual summary of the document indicative of the report, even though it may also appear elsewhere in the body of the technical report. If additional space is required, a continuation sheet shall be attached.

It is highly desirable that the abstract of classified reports be unclassified. Each paragraph of the abstract shall end with an indication of the military security classification of the information in the paragraph, represented as *(TS), (S), (C), or (U)*.

There is no limitation on the length of the abstract. However, the suggested length is from 150 to 225 words.

14. KEY WORDS: Key words are technically meaningful terms or short phrases that characterize a report and may be used as index entries for cataloging the report. Key words must be selected so that no security classification is required. Identifiers, such as equipment model designation, trade name, military project code name, geographic location, may be used as key words but will be followed by an indication of technical context. The assignment of links, rules, and weights is optional.

OBJECTIVE

Analyze the performance of tires in soft soils.

RESULTS

An equation relating the drawbar-pull exerted by a wheel operating in soft soil has been derived as a function of slip.

CONCLUSIONS

The optimum drawbar-pull is reached at a sinkage which corresponds to that point of the wheel perimeter which has a vertical instantaneous-velocity vector.

ADMINISTRATIVE INFORMATION

This program was supervised and conducted by the Land Locomotion Laboratory of ATAC under D/A Project No. 597-01-006, Project No. 5016.11.84400.

TABLE OF CONTENTS

ABSTRACT

This report presents the first semi-empirical solution suggested to describe the traction versus slip relationship for rigid wheels.

The kinematics of a slipping wheel are analyzed and the results are used to express the shear deformation as a function of slip which in turn is utilized in a new shear stress-strain relationship. The shear stresses are expressed at every point of the tire-soil interface surface and integrated to obtain the traction.

Other established information is also briefly discussed, in order to complete the description of the state-of-the-art.

DEFINITIONS, SYMBOLS

R	Motion Resistance (Lbs.)
N	Normal Component of the Resultant Soil Reaction (Lbs.)
T	Tangential Component of the Resultant Soil Reaction (Lbs.)
α_o	Central Angle Associated with the Resultant Soil Reaction (o)
W	Vertical Load on the Wheel Axis (Lbs.)
D	Diameter of the Wheel (in.)
M_b	Moment Due to Bearing Friction (inch Lbs.)
ϱ_f	Factor of Bearing Friction
z	Vertical Distance between a Point on the Wheel Perimeter and the Undisturbed Ground Level (in.)
z_o	Sinkage of the Wheel (in.)
β_o	Central Angle Associated with Z_o (o)
p	Pressure (stress) Normal to the Boundary (Lbs./in.^{2})
k_c	Cohesive Modulus of Sinkage (Lbs/in.$^{n+1}$)
k_ϕ	Frictional Modulus of Sinkage (Lbs/in.$^{n+2}$)
n	Exponent of Sinkage
α	Central Angle Associated with Z
Θ	$2\pi - \alpha$
M	Net Torque Applied to Drive the Wheel (inch Lbs.)
DP	Drawbar Pull, Net Traction (Lbs.)
V_s	Velocity of Slipping (in./sec.)
i_o	Slip
V_t	Theoretical Velocity of the Wheel (in./sec)

ω	Angular Velocity of the Wheel (Rad/sec)
v_x	Horizontal Component of the Velocity Vector at A Point on the Wheel Perimeter Associated with V = ωt (in./sec)
v_y	Vertical Component of the Velocity Vector at a Point on the Wheel Perimeter Associated with V = ωt(in./sec)
C	Instantaneous Center of Motion
r	Rolling Radius (in.)
y_c	Ordinate of C (in.)
$\bar{I}$	Unit Vector in X Direction (in./sec)
$\bar{j}$	Unit Vector in y Direction (in./sec)
β	Angle Enclosed by the Velocity Vector and the X Axis (o)
Θ_v	Central Angle Associated with the Point of the Wheel at which the Velocity Vector is Vertical.
$\bar{a}$	Acceleration Vector (in./sec^2)
ϱ	Radius of Curvature (in.)
s_{max}	Shear Strength of the Soil (Lbs./in.^{2})
c	Cohesion (Lbs./in.^{2})
ϕ	Angle of Internal Friction
α_f	Angle of Failure (o)
s	Shear Stress (Lbs./in.^{2})
j	Shear Deformation (in.)
K	Tangent Modulus of a Shear Stress Strain Curve (in.)

LIST OF FIGURES

Figure No.

Figure No.

INTRODUCTION

The problems related to rigid wheel behavior in soft soil were first analyzed by Bernstein [1]. He derived relationships between the load on a towed wheel of given geometry and the sinkage as well as the motion resistance. The basic assumption employed by Bernstein was that the normal soil stress acting on the wheel surface is proportional to the square root of the vertical distance of the point in question and the ground level. Thus, the influence of the soil on the stress distribution was accounted for by a factor of proportionality (k). Russian agricultural engineers have introduced another "soil characteristic" by using a general exponent (n) instead of the square root.[2]. Most of the Russian publications, however, follow Gerstner by assuming n = 1, to avoid mathematical complications which arise from the non-integer exponent. In 1950, Garbari [3], published a very useful paper in which he suggested some new notions such as the "critical inflation pressure".

A further development in the adaptability of the empirical pressure distribution equation was accomplished by Bekker[4], who suggested a new factor of proportionality which is practically independent of the size of the penetrometer footing, or that of the wheel-soil interface if the aspect

ratio is not allowed to be less than 5:1. Bekker rederived Bernstein's equations using the new soil value system [5].

Vincent [6], and more recently Hegedus [7], observed some new relationships as to the normal pressure distribution under a wheel, but no method has been devised as yet to describe it analytically.

Tanaka [8], and Phillips [9], analyzed the equilibrium of wheels in their presentations at the First International Conference on the Mechanics of Soil-Vehicle Systems. Both of the authors included the tangential forces, hitherto neglected.

Uffelmann conducted tests [10], by means of a special apparatus enabling him to measure the tangential "rim stresses" and suggested a simple plastic theory of rut formation providing an estimate of rolling resistance. His equations are equal to Bekker's equations for zero exponent, or in other words, they are valid for bearing capacity estimations (zero sinkage). Therefore, no conclusions as to the sinkage may be obtained on this basis.

An excellent analysis of the equilibrium of wheels by Schuring also stresses the importance of the tangential forces [11]. In addition, it dwells on the possibility of using dimensionless analysis techniques for the wheel problem.

The latter approach has also been elaborated on by Hicks and Nuttal at the First International Conference (12 and 13).

The kinematics of a rigid wheel and that of a soil particle were analyzed by Andreyev[14], and other Russian investigators in great detail. Their basic assumption, however, that the displacement of a soil particle and the force acting on it are collinear is incorrect and leads to certain ranges on the wheel perimeter according to slip conditions which are questionable on the basis of test results obtained by Vincent and Uffelmann. As for soft tires, Omelyanov's empirical equation for resistance prediction is frequently published in Russian textbooks [15].

Another Russian paper by Ageykin [16], reveals an equation for sinkage similar to that published by Bekker and the writer [17, 18, 19, 20].

Experiments by the National Tillage Laboratory [21], by the Waterways Experiment Station of the Corps of Engineers, U. S. Army [22], by Soehne [23], and by a group consisting of researchers from the National Tillage Laboratory and Michigan State University [24], elucidated some important aspects of the pressure distribution under soft tires operating in deformable soils.

Kerr [25], and Chapoux [26], carried out extensive research projects on tire behavior in sand. Weinblum and Orlowski [27], as well as other Israelian researchers are also engaged in investigating wheels in sandy soils. They found that an exponential expression is suitable to describe the traction slip relationship. Soehne and Sonnen [28] arrived at the same approximation in their broad experimental studies presented in Turin. They emphasized the difficulties which arose with the application of the Bekker soil value system in multi-layer soils.

Turnbull and Freitag accounted for a massive tire test program which is being conducted at the Waterways Experiment Station [29]. The authors investigate the change in performance due to multiple passes, beside the traction-slip problem.

A new, radial ply, tire design, introduced by the Pirelli Company [30], proved to be superior to the conventional one, according to tests conducted by the Company itself, by the National Tillage Laboratory [31], and by the Ford Motor Co. [32].

Bekker's condual tire concept appeared to be promising, in view of theoretical considerations and some limited test results [33]. Richey suggested the mounting of a radial ply tire on a narrow rim. The idea proved to be advantageous over a conventional rim equipped with a radial ply tire [32].

Various aspects of tire behavior on hard ground have been analyzed by a great number of researchers and institutions. An excellent, if not quite up-to-date, digest of these studies has been published by Hadekel[34].

OBJECT

The purpose of this research project was the establishment of simple equations based on empirical soil stress-strain relationships which would enable one to predict the sinkage, the motion resistance, and the traction of a rigid wheel and a soft tire. While there have been empirical solutions suggested for the first two problems, the question of traction of wheels has not been evolved farther than the statement that the tractive force is the sum of the horizontal components of the stresses acting along the soil-wheel interface surface. A number of researchers have stated that a rigorous solution represents an impossible task at present. This is probably true, since the basic theory of soil mechanics has failed to answer such basic questions as the true stress-strain relationship prevailing under a plate. No wonder that a solution for the involved three-dimensional problem of a tire-soil interaction, in which the behavior of the carcass, and the effect of the lugs[35] represent even further obstacles in the analysis, has not been considered obtainable. Nevertheless it is felt that adequate empirical knowledge is available on soil behavior to make our goal feasible.

SUMMARY

Exact equations of equilibrium for driven wheels operating in soft soil are presented for which a formula for motion resistance is derived.

Next a detailed analysis of the kinematics of a slipping wheel is presented and a geometric representation of the velocity distribution is introduced.

An empirical soil shear stress-deformation equation is proposed. This equation is then combined with the results of the previous analysis and an equation for the gross traction of a tire is derived.

CONCLUSIONS

The theoretical investigation leads to the following conclusions:

The perimeter of the wheel may generally be divided into four regions depending on the direction of the velocity vectors that belong to the pertinent points.

When the sinkage is such that the region characterized by vectors pointing forward and downward is a part of the wheel-soil interface (in case of driven wheels) the tangential stresses result in resisting forces. Hence, optimum traction is reached when the sinkage is not greater than the height of the point to which a vertical velocity vector belongs.

RECOMMENDATIONS

It is recommended that the theoretical method presented in this paper be thoroughly checked by a series of experiments to establish its applicability and its limitations

THEORETICAL ANALYSIS

The tire may be considered rigid if the inflation pressure is higher than the so-called critical pressure (defined in Part II).

To express the sinkage and the motion resistance of a towed wheel operating in soft ground, consider Figure 1:

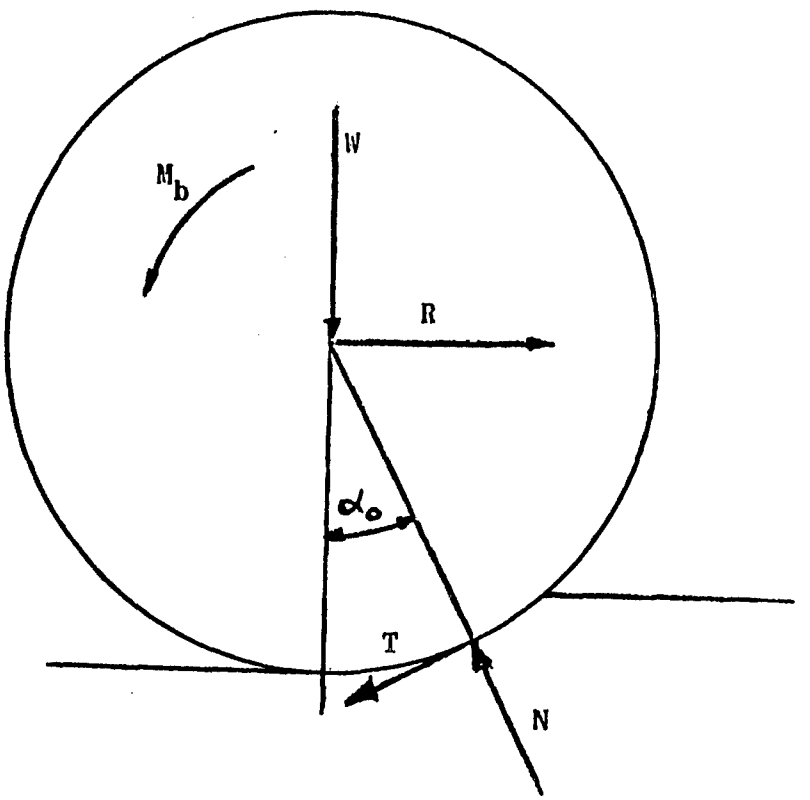

Figure 1.

It is assumed that the problem is two dimensional. The equations of equilibrium are the following:

$$R - N \sin \alpha_o + T \cos \alpha_o = 0 \quad \ldots\ldots\ldots (1\text{-a})$$

$$W + T \sin \alpha_o - N \cos \alpha_o = 0 \quad \ldots\ldots\ldots (1\text{-b})$$

$$T \frac{D}{2} - M_b = 0 \quad \ldots\ldots\ldots (1\text{-c})$$

where $M_b = W\delta_1$ naturally.

Thus, the magnitude of T can be found if W and δ are known. (Equation 1-c). The tangential component of the resultant is a function of slip. This relationship will be derived on page 38. Thus, it is theoretically possible to establish the magnitude of the negative slip which occurs under a towed wheel.

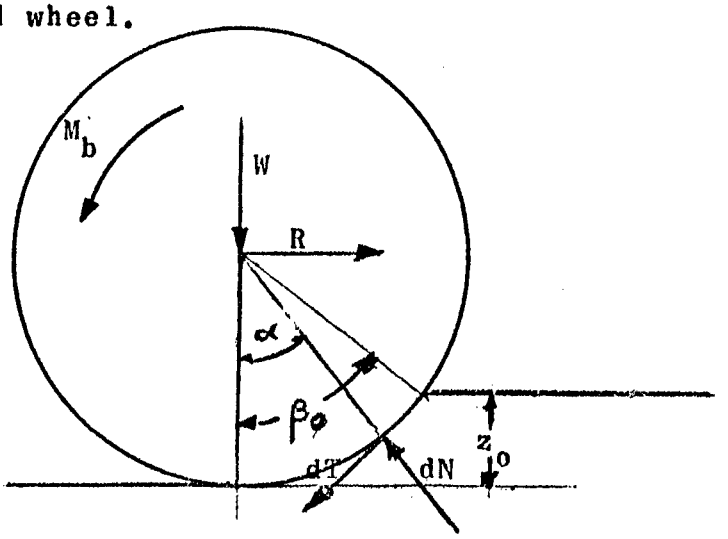

Figure 2.

Equation (1) may be rewritten as follows:

$$R - \int_0^{\beta_0} d\,T \cos\alpha - \int_0^{\beta_0} dN \sin\alpha = 0 \quad \ldots \quad (2a)$$

$$W - \int_0^{\beta_0} dN \cos\alpha + \int_0^{\beta_0} d\,T \sin\alpha = 0 \quad \ldots \quad (2b)$$

$$\frac{D}{2} \int_0^{\beta_0} dT - M_b = 0$$

Thus, if $dT = f(\alpha)$ and $dN = g(\alpha)$ is known the sinkage and the motion resistance may be found.

Note that:

$$z_0 = \frac{D}{2}(1 - \cos\beta_0) \quad \ldots \quad (3)$$

Bekkers approximative equation will be used throughout this paper for:

$$p = \frac{dN}{dA} = f(z) = g(\alpha) = h(\theta)$$

$$p = \left(\frac{k_c}{b} + k_\phi\right) z^n = \left(\frac{k_c}{b} + k_\phi\right)\left[(\cos\theta - \cos\beta_0)\frac{D}{2}\right]^n \quad \ldots \quad (4)$$

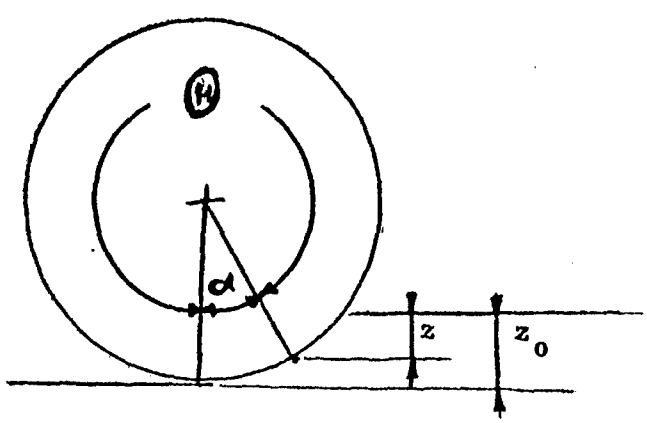

Fig. 3

If one assumes that M_b is negligible, then $T = 0$ and

$$R = \int_0^{\beta_0} dN \sin\alpha = -\int_{2\pi}^{2\pi-\beta_0} dN \sin\theta \quad . \quad . \quad . \quad . \quad (5)$$

Using equation (4):

$$R = \frac{bD}{2} = \left(\frac{k_c}{b} + k_\phi\right) \int_{2\pi-\beta_0}^{\beta_0} \left[\frac{D}{2}(\cos\theta - \cos\beta_0)\right]^n \sin\theta \, d\theta$$

$$= b\left(\frac{k_c}{b} + k_\phi\right)\left(\frac{D}{2}\right)^{n+1} \left[1 - \cos\beta_0\right]^{n+1} \frac{1}{n+1}$$

From equation (4):

$$1 - \cos\beta_0 = \frac{z_0}{D/2}$$

Thus:

$$R = \frac{k_c + b\,k_\phi}{n+1} z_0^{\,n+1} \quad . \quad . \quad . \quad . \quad . \quad . \quad . \quad . \quad . \quad . \quad (6)$$

Equation 6 was first derived by Bekker[5], using energy considerations. It enables one to approximate the rolling resistance of a towed wheel for small slippages only because the tangential forces have been neglected.

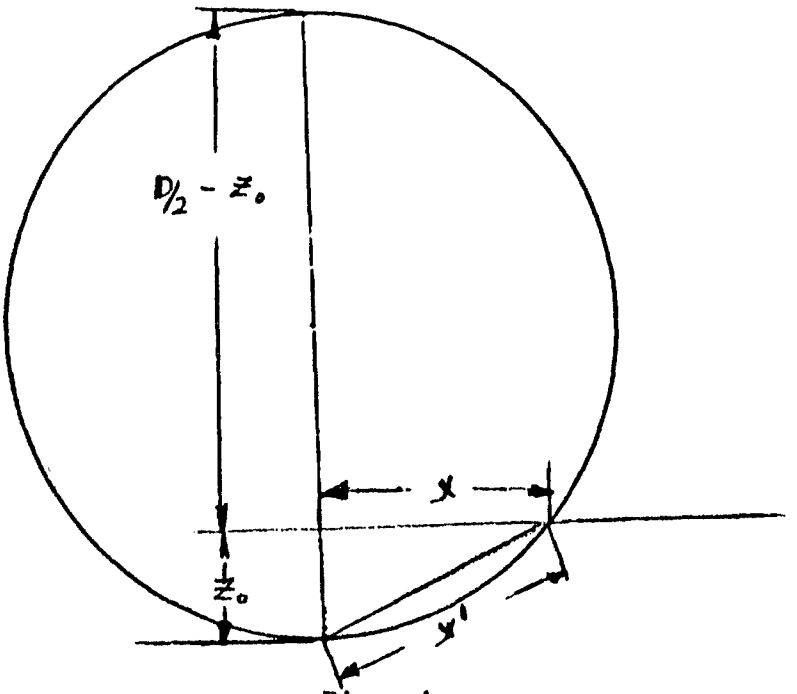

Fig. 4

Bekker and Hegedus have attempted to remedy this shortcoming by introducing the so-called bulldozing resistance. (5) (37).

Equation (2b) cannot be solved in a closed form even if one assumes dT = 0 for all A. Bekker has performed the integration [5] by neglecting the difference between x and x', (Fig. 4) and by considering the first two terms in the binominal series of

$$[1 - (Z_o - Z)]^n$$

Ehrlich [36] improved the accuracy of Bekker's solution by considering three terms in the series. He found that the accuracy is a function of n. Bekker's solution yields the following equation:

$$z_o = \left[\frac{3\,W}{(3-n)(k_c + bk_\phi)\sqrt{D}} \right]^{\frac{2}{2n+1}} \quad \ldots\ldots 7$$

Since $n \leq 2$, according to actual measurements, $n = 3$ is excluded by practical considerations. Erhlich's equation reads as follows:

$$z_o = \left[\frac{W}{bk\sqrt{D'}} \right]^{\frac{2}{2n+1}} \left[(1-.51\,n+.22n^2) - \frac{2}{D}(.25-.26n-.14n^2) \left(\frac{W}{bk\sqrt{D}(1-.51n+.22n^2} \right)^{\frac{2}{2n+1}} \right]^{\frac{-2}{2n+1}} \quad \ldots\ldots 8$$

Equation 1, may be rewritten for a driven wheel as follows: (Figure 5):

$$\int_{2\pi-\beta_o}^{2\pi} dT \cos\theta + \int_{2\pi-\beta_o}^{2\pi} dN \sin\theta - R = 0 \quad \ldots (9\text{-a})$$

$$W + \int_{2\pi-\beta_o}^{2\pi} dT \sin\theta - \int_{2\pi-\beta_o}^{2\pi} dN \cos\theta = 0 \quad \ldots (9\text{-b})$$

$$M - \frac{D}{2} \int_{2\pi-\beta_o}^{2\pi} dT = 0 \quad \ldots\ldots\ldots (9\text{-c})$$

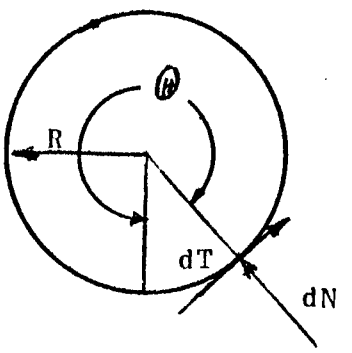

Figure 5.

Here R is called the drawbar pull (DP), and dN sin θ is considered to be the motion resistance. Later it will be shown, however, that a part of dT cos θ is a resisting force also in many cases.

In order to evaluate dT as a function of H, one has to analyze the kinematics of a rigid wheel.

KINEMATICS OF A RIGID WHEEL

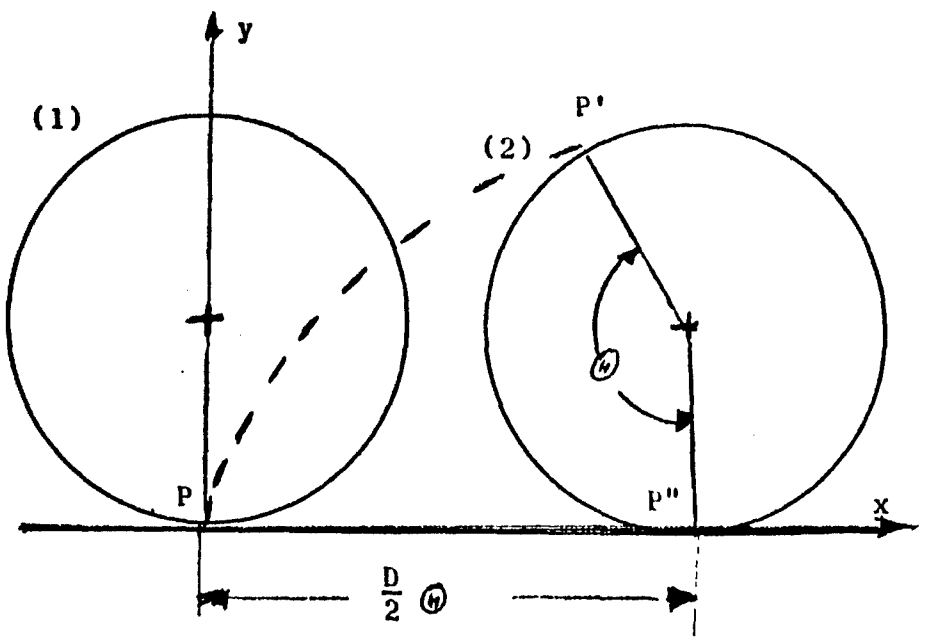

Figure 6.

As the wheel moves from position 1 to position 2, while turning by an angle Θ point, "P" is transferred to "P'", Fig. 6. The path of the point is called a cycloid and its parametric equation is the following:

$$x = \frac{D}{2}(\theta - \sin\theta) \quad \ldots\ldots\ldots\ldots\ldots \quad (10a)$$

$$y = \frac{D}{2}(1 - \cos\theta) \quad \ldots\ldots\ldots\ldots\ldots \quad (10b)$$

Equation 10 is valid if no slip occurs between the horizontal plane (x axis) and the wheel perimeter. In case of slip $\overline{PP''}$ is no longer equal to $(D/2)\Theta$.

The relative velocity between the fixed x axis and the bottom of the wheel (v_s) determines the slip as follows:

$$i_o = -\frac{v_s}{v_T} \quad \ldots\ldots\ldots\ldots\ldots\ldots \quad (11)$$

It can be seen that i_o is positive if v_s and v_T are of opposite sense (driven wheel). The theoretical velocity (v_T) is defined by:

$$v_T = \frac{D}{2}\omega = \frac{D}{2}\frac{\Theta}{t} \quad \ldots\ldots\ldots \quad (12)$$

Thus:

$$\overline{PP''} = \frac{D}{2}\Theta + v_s t = \frac{D}{2}\Theta - i_o v_T t$$

$$= \frac{D}{2}\Theta(1 - i_o) \quad \ldots\ldots\ldots\ldots \quad (13)$$

Thus, the equation of the path becomes:

$$x = \frac{D}{2}\left[\Theta\,(1-i_o) - \sin\theta\right] \quad \ldots\ldots\ldots \quad (14a)$$

$$y = \frac{D}{2}\,(1 - \cos\theta) \quad \ldots\ldots\ldots \quad (14b)$$

Denote

$$r = \frac{D}{2}\,(1 - i_o) \quad \ldots\ldots\ldots\ldots \quad (15)$$

Then

$$x = r\theta - \frac{D}{2}\sin\theta \quad \ldots\ldots\ldots\ldots \quad (16a)$$

$$y = \frac{D}{2}\,(1 - \cos\theta) \quad \ldots\ldots\ldots\ldots \quad (16b)$$

or using $\theta = \omega t$

$$x = \frac{D}{2}\left[\omega t(1 - i_o) - \sin(\omega t)\right] \ldots\ldots \quad (17a)$$

$$y = D/2\,(1 - \cos\omega t) \quad \ldots\ldots\ldots \quad (17b)$$

or

$$x = r\omega t - \frac{D}{2}\sin(\omega t) \quad \ldots\ldots\ldots \quad (18a)$$

$$y = D/2\,(1 - \cos\omega t) \quad \ldots\ldots\ldots \quad (18b)$$

The parametric equation of the velocity vector is:

$$v_x = \dot{x} = \frac{dx}{dt} = \frac{D}{2}\,\omega\left[(1 - i_o) - \cos(\omega t)\right] \ldots (19a)$$

$$v_y = \dot{y} = \frac{dy}{dt} = \frac{D}{2}\,\omega\,\sin\omega t \quad \ldots\ldots\ldots \quad (19b)$$

Or

$$v_x = \omega\left[r - \frac{D}{2}\cos\omega t\right] \quad \ldots\ldots\ldots \quad (20)$$

When $\Theta = \omega t = 0 \text{ or } 2\pi$

$$v_x = \omega(r - D/2) = -\omega D/2\, i_o = -v_T\, i_o = v_s \quad \ldots \quad (21a)$$

$$v_y = 0 \quad \ldots \quad (21b)$$

Thus at the bottom of the wheel, the velocity is equal to v_s. The speed or the absolute value of the velocity is:

$$| \bar{v} | = \sqrt{\dot{x}^2 + \dot{y}^2} = \frac{D}{2}\omega \left[4 \sin^2 \left(\frac{\omega}{2} t\right)(1 - i_o) + i_o^2 \right]^{\frac{1}{2}} \quad \ldots \quad (22)$$

For $i_o = 1$; $| \bar{v} | = \frac{D}{2} w$

For $i_o = 0$; $| \bar{v} | = D\omega \sin \left(\frac{\omega}{2} t\right)$ $\quad \ldots \quad (23)$

Imagine that the entire xy plane is rigidly attached to the wheel. There exists a point in the plane where velocity is zero. This point is called the instantaneous center of motion (C). It can be seen that C must lie on the vertical line of symmetry. (Equation 21). Every point in the revolving and translating plane may be thought of as being on the perimeter of a wheel of radius $(D/2)^*$. From Equation 20:

$$v_x = \omega\left[r - (D/2)^*\right] = 0$$

when $(D/2)^* = r = D/2(1 - i_o)$ $\quad \ldots \quad (24)$

Thus $y_c = D/2 - D/2(1 - i_o) = D/2\, i_o$ $\quad \ldots \quad (25)$

Hence, $r = (1 - i_o)\, D/2$, is the radius of an imaginary wheel which is attached to the actual wheel and has no slip at its bottom, which is at C. $D/2(1 - i_o) = r$, is often called the rolling radius.

In case of driven wheels, $v_s < 0$. Thus, $i_o > 0$, $r < D/2$, and $y_c > 0$, which means that the instantaneous center is above the x axis. For $i_o = 1$ (100% slip), $r = 0$, or $y_c = D/2$. Thus C coincides with the center of the wheel. For towed wheels, $v_s > 0$, $i_o < 0$, $r > D/2$ and $y_c < 0$

$$\text{since} \quad r = D/2(1 + |i_o|) \quad \ldots\ldots\ldots\ldots \quad (26)$$

C is below the x axis.

For $i_o = 1$ (100% negative slip)

$$r = 2\, D/2 = D$$

Consequently, $i_o = -100\%$ does not represent a completely blocked wheel. When $i_o \to -\infty$, $v_T \to o$, $r \to \infty$, or $y_c \to -\infty$, which means that the wheel slides on the ground without turning. (When $v_T \to o$, $\omega \to o$, since $v_T = \omega t$). It is not advisable to use two different definitions for the slip, as is generally done, depending on whether one deals with driven or towed wheels, because the mathematics cannot be kept completely general. In other words, if one defines negative slippage so that it becomes -100% when the wheel is blocked, so that

$$i_c = -\frac{v_s}{v_T + v_s}$$

then the case of towed wheel cannot be handled with the same set of equations derived for driven wheels.

An interesting geometric representation of the velocity vector distribution along the wheel perimeter is presented in the following. Construct a circle of radius $D/2\omega$ so that the abscissa of its center be $x = r\omega = D/2\ (1 - i_o)\omega$ and its ordinate be zero, Figure 7.

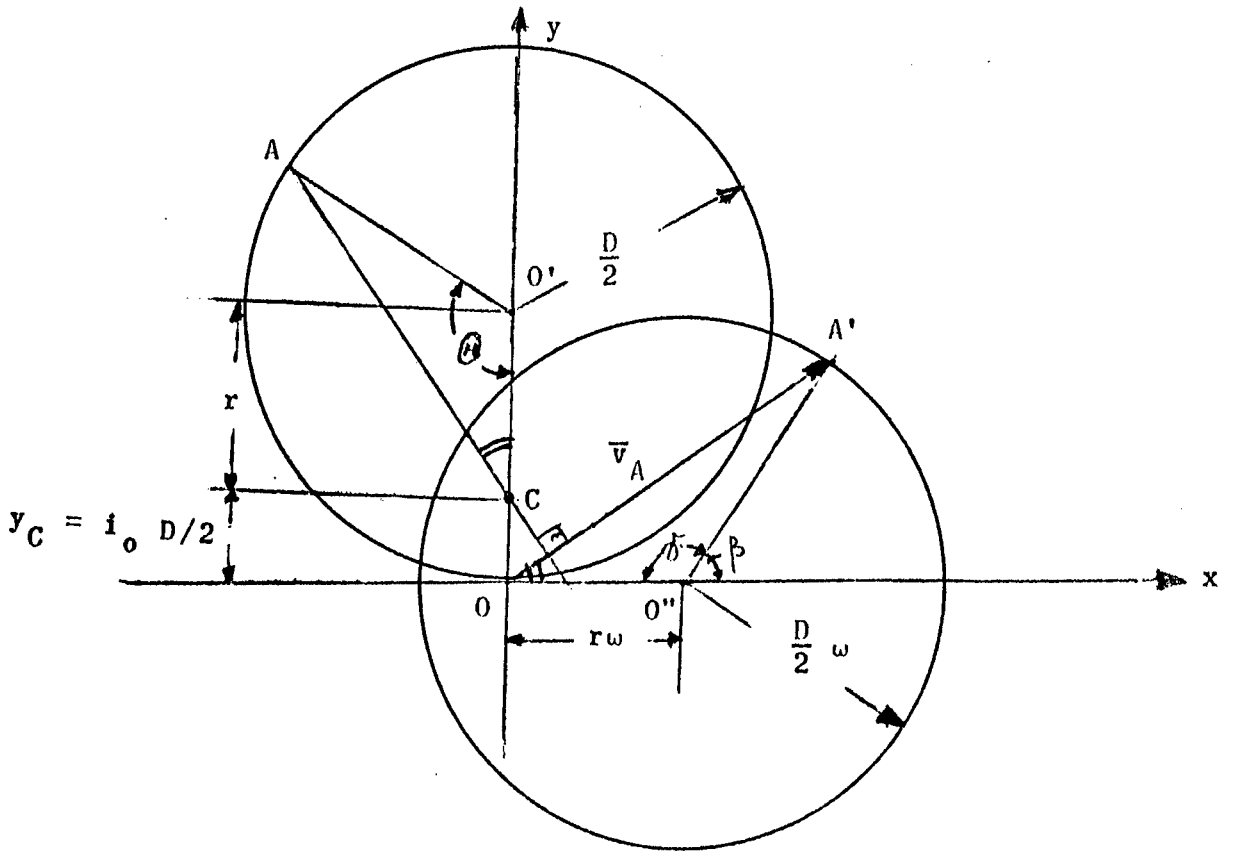

Figure 7.

The velocity vector associated with an arbitrary point A on the wheel perimeter can be found as follows:

a. Connect A and C

b. Draw a line perpendicular to $\overline{AC}$ through O

The line segment $\overline{OA'}$ represents the velocity vector at A.

Proof: $\overline{v_A} = (r\omega + D/2\ \omega \cos\beta\ )\ \overline{i} + R\ \omega \sin\beta\ \overline{j}$

but $\cos\beta = -\cos\gamma = -\cos\theta$

$\sin\beta = \sin\theta$

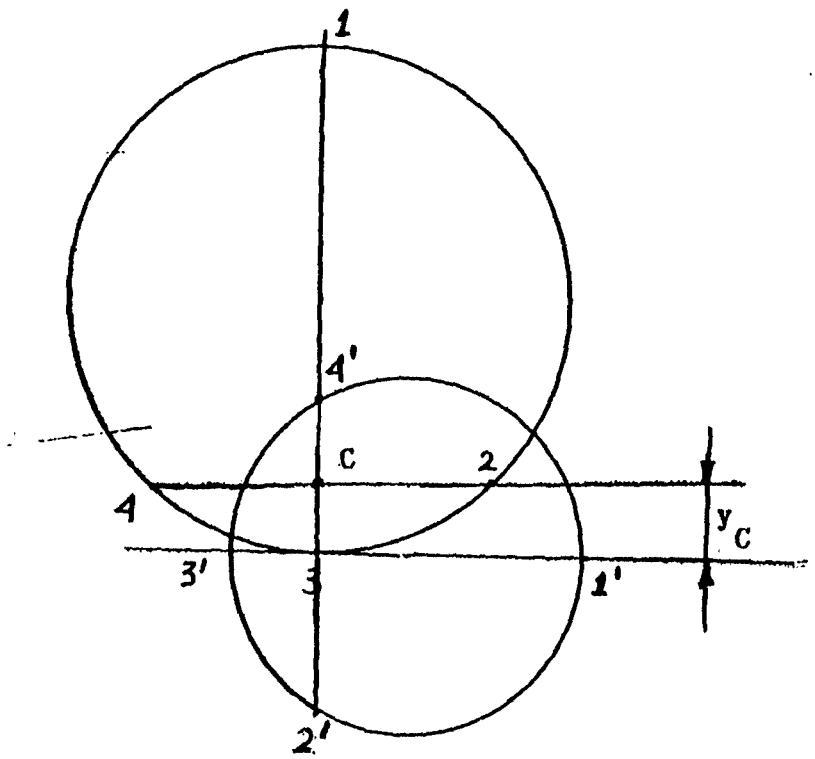

Figure 8

Hence $\overline{v_A} = (r\omega - D/2\ \omega \cos\theta)\ \overline{i} + D/2\ \omega \sin\theta\ \overline{j}$ . . (27)

Equation 27 is equal to equation 19 or 20, Q.E.D. (To see that $\theta = \gamma$ consider the triangles AO'C and OO"A'. Two of their sides are proportional, D/2, r and D/2 ω, r ω and one of their angles is equal. Hence the triangles are similar, thus all three angles are equal).

It can, therefore, be concluded that the circle constructed is the hodograph of the path.

DRIVEN WHEELS:

The wheel perimeter may be divided into four regions according to the "behavior" of the velocity vectors.

Region 1: The velocity vectors point up and to the right along Section $\widehat{41}$ (Fig. 8).

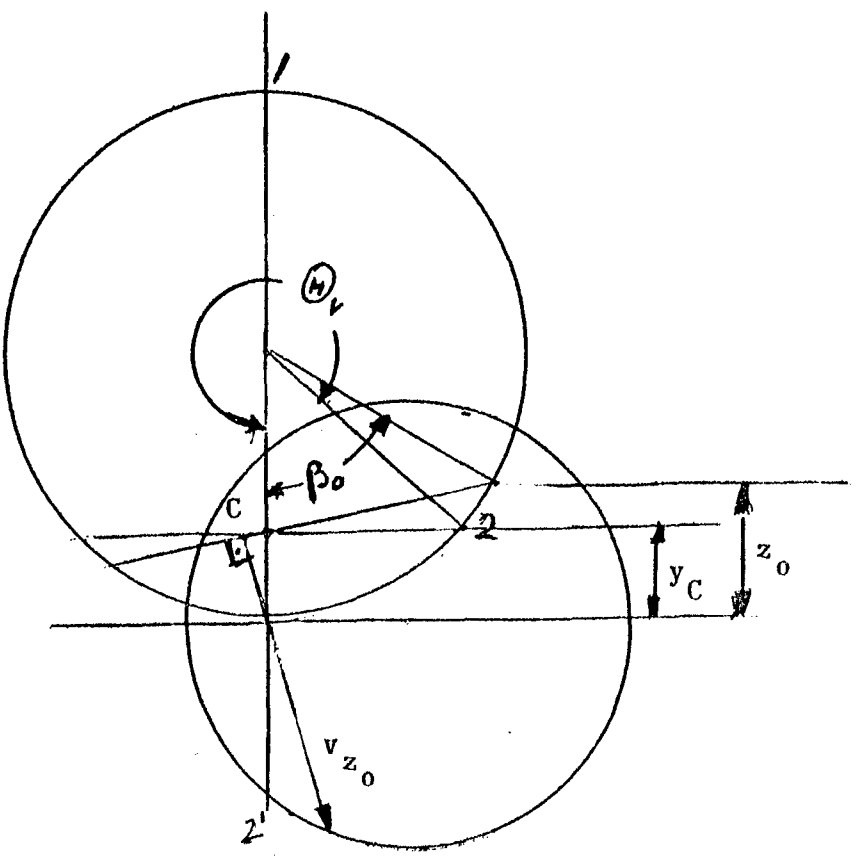

Figure 8a.

Region 2: The velocity vectors point downward and to the right on Section $\overset{\frown}{12}$ Therefore, if the sinkage of the wheel z_o is such that $z_o > y_c$ positive horizontal deformation and compaction is imparted on the soil along the section associated with $z_o - y_c$. The point on the wheel perimeter whose ordinate is y_c belongs to an angle $\Theta_v = \cos^{-1}(1 - i_o)$, because (from Equation 19a) $v_x = o$ when $\omega t = \Theta = \cos^{-1}(1 - i_o)$. Thus, the region characterized by $z_o - y_c$ may also be defined as follows:

$$2\pi - \beta_o \leq \Theta \leq \Theta_v$$

or from Equation 3:

$$2\pi - \cos^{-1}(1 - \frac{2z_o}{D}) \leq \Theta \leq \cos^{-1}(1 - i_o)$$

The tangential forces acting on the wheel in Region 2 have negative horizontal components, thus an additional resistance will occur. The sum of these tangential forces has been denoted H_2 (38). Note that Region 2 is important only when

$$2\pi - \beta_o \leq \Theta_v = \cos^{-1}(1 - i_o)$$

Thus, the sinkage and the slip has to satisfy the above inequality when $H_2 \neq 0$.

Region 3: The velocity vectors point downward and to the left along Section $\overset{\frown}{23}$ Compaction and positive horizontal shear stress components occur here when the wheel is driven. The section of the wheel perimeter along which

positive shear stresses (tractive forces) occur is defined by β_o. When $2\pi - \beta_o \leq \Theta_v$ this section becomes the entire arc $\overset{\frown}{23}$

Region 4: Here the velocity vectors point upward and to the left. Neglecting the small recovery effect of soils this region is of no importance, since the wheel is not in contact with the ground along arc $\overset{\frown}{34}$.

Zero Slip: For zero slip, $r = D/2(1 - i_o) = D/2$. The hodograph is tangent to the y axis. (Fig. 9). (C is at O). There are no velocity vectors with negative horizontal components. Hence, traction cannot be developed.

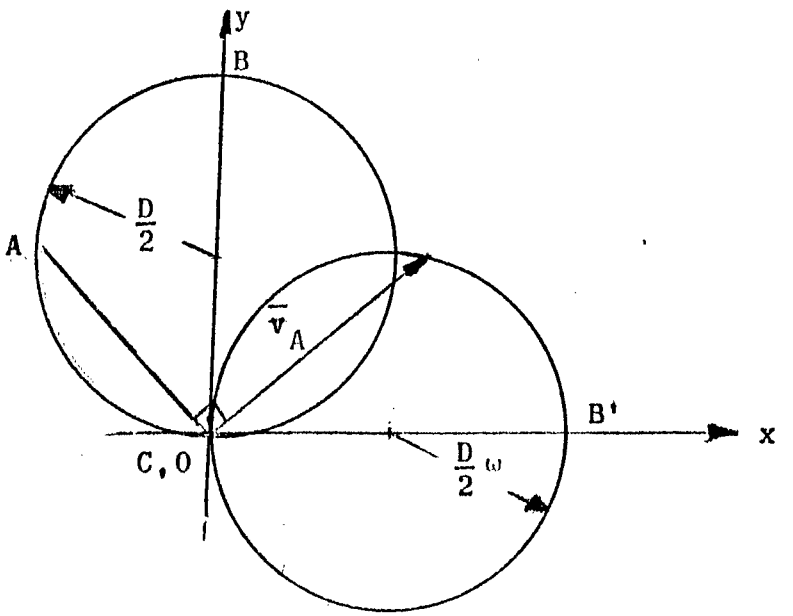

Fig. 9

There are two regions only. The velocity vectors along $\overset{\frown}{OB}$ point upward and to the right, while along $\overset{\frown}{BO}$ the vectors point downward and to the right.

Negative Slip: For negative slip, the diagram is shown in Fig. 10. There are two regions as in the no-slip case, but $v = v_s$ at the bottom of the wheel.

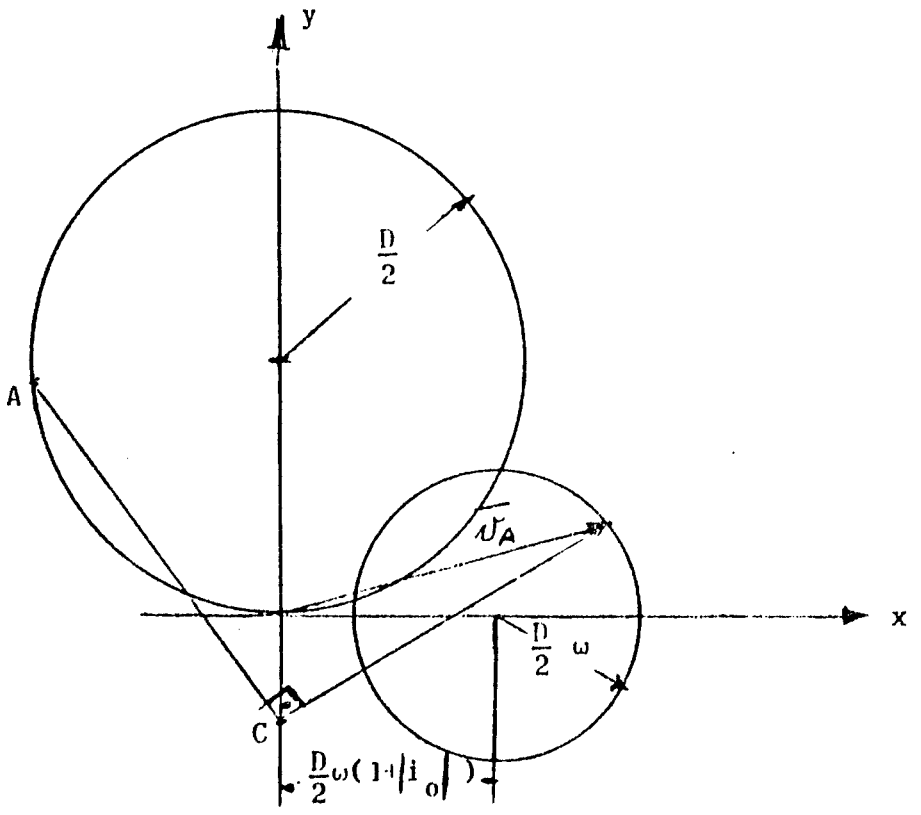

Fig. 10

Acceleration:

The acceleration of a point located on the wheel perimeter may be obtained from Equations 19a and b.

$$a_x = \ddot{x} = \frac{d^2x}{dt^2} = \frac{dv_x}{dt} = D/2\ \omega^2 \sin \omega t \quad . . \quad (28a)$$

$$a_y = \ddot{y} = \frac{d^2y}{dt^2} = \frac{dv_y}{dt} = D/2\ \omega^2 \cos \omega t \quad . . . \quad (28b)$$

Note that the acceleration is independent from the slip. It can be seen that the endpoints of the acceleration vectors describe a circle of radius $D/2\ \omega^2$. The magnitude of the acceleration

$$\left|\bar{a}\right| = \sqrt{a_x^2 + a_y^2} = D/2\ \omega^2 \text{ is constant.}$$

Its direction is parallel to the radius and its sense points toward the center of the wheel, just as in the case of a uniform circular motion.

The radius of curvature is:

$$\rho = \frac{(\dot{x}^2 + \dot{y}^2)^{3/2}}{\begin{vmatrix} \dot{x} & \dot{y} \\ \ddot{x} & \ddot{y} \end{vmatrix}} \quad . . . . . \quad (29)$$

For

$$i_o = 0 \qquad \rho = 2\ D \sin \left(\frac{\omega}{2} t\right) \quad . . . . . \quad (30)$$

Thus

$$\rho = 2\ \overline{AC}$$

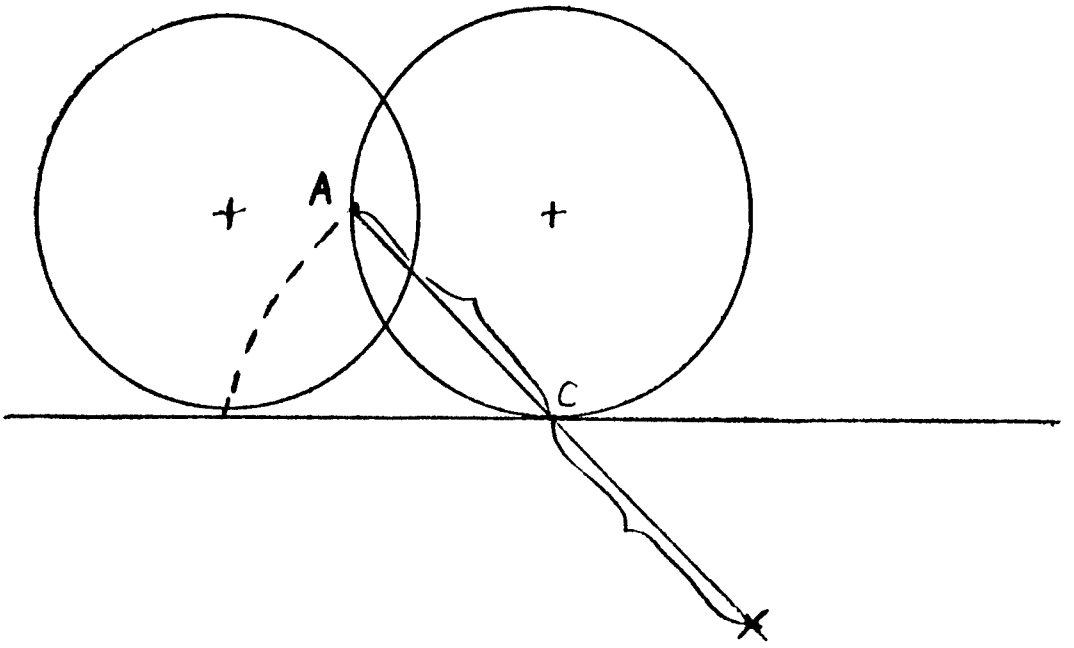

Fig. 11

When $i_o \neq 0$; $\varrho = \dfrac{D/2\,[4\sin^2(\frac{\omega}{2}t)(1 - i_o) + i_o^2]^{3/2}}{2\sin^2(\frac{\omega}{2}t)(1 - i_o) + i_o}$ . . . (31)

A comparison of Equations 23 and 30 reveals that:

$$|\bar{v}| = 1/2\,\varrho\,\omega \quad \text{for } i_o = 0$$

The tangential component of the acceleration is:

$$|\bar{a}_T| = \frac{d\,|\bar{v}|}{dt} = \frac{D/2\,\omega^2(1 - i_o)\sin(\omega t)}{[4\sin^2(\frac{\omega}{2}t)(1 - i_o) + i_o^2]^{1/2}} \quad . . . (32)$$

for $i_o = 0$

$$|\bar{a}_T| = D/2\ \omega^2 \cos(\tfrac{\omega}{2} t) \quad \ldots\ldots\ldots\ldots (33)$$

for $i_o = 1$

$$|\bar{a}_T| = 0$$

The normal component of the acceleration is

$$|\bar{a}_N| = \frac{|\bar{v}^2|}{\rho} = \frac{D}{2}\omega^2 \frac{2 \sin^2(\frac{\omega}{2} t)(1 - i_o) + i_o}{[4 \sin^2(\frac{\omega}{2} t)(1 - i_o) + i_o^2]^{1/2}} \quad \ldots (34)$$

for $i_o = 0$

$$|\bar{a}_N| = \frac{D}{2}\omega^2 \sin(\tfrac{\omega}{2} t) \quad \ldots\ldots\ldots\ldots (35)$$

for $i_o = 1$

$$|\bar{a}_N| = \frac{D}{2}\omega^2 = \frac{|\bar{v}|^2}{D/2}$$

From Equations 32 and 34

$$|\bar{a}| = \sqrt{|\bar{a}_N|^2 + |\bar{a}_T|^2} = \frac{D}{2}\omega^2 \quad \ldots\ldots (36)$$

This checks with Equations 28a and b. Thus, when the wheel moves with constant speed (ω = const) the acceleration vectors are not different from that of uniform circular motion.

SHEAR STRESS STRAIN RELATIONSHIP

The next task is to establish a shear stress-strain relationship which allows one to describe an experimental soil

shear curve by means of coefficients, which depend on the soil and its state. (Moisture content, density, load history, etc.).

The soil shear strength was first expressed by Coulomb[39], as follows:

$$s_{max.} = c + p \tan \phi \quad \ldots\ldots\ldots\ldots \quad (37)$$

The numerical values of c and ϕ may be obtained by triaxial tests or by direct shear test. The well known triaxial test procedure is as follows[40]. A cylindrical soil speciman is subjected to p_1 axial stress and p_3 radial stress.

Mohr's diagram, Figure 12, represents the stresses acting on a plane which inclosed $(\frac{\pi}{2} - \alpha)$ angle with the axis of symmetry.

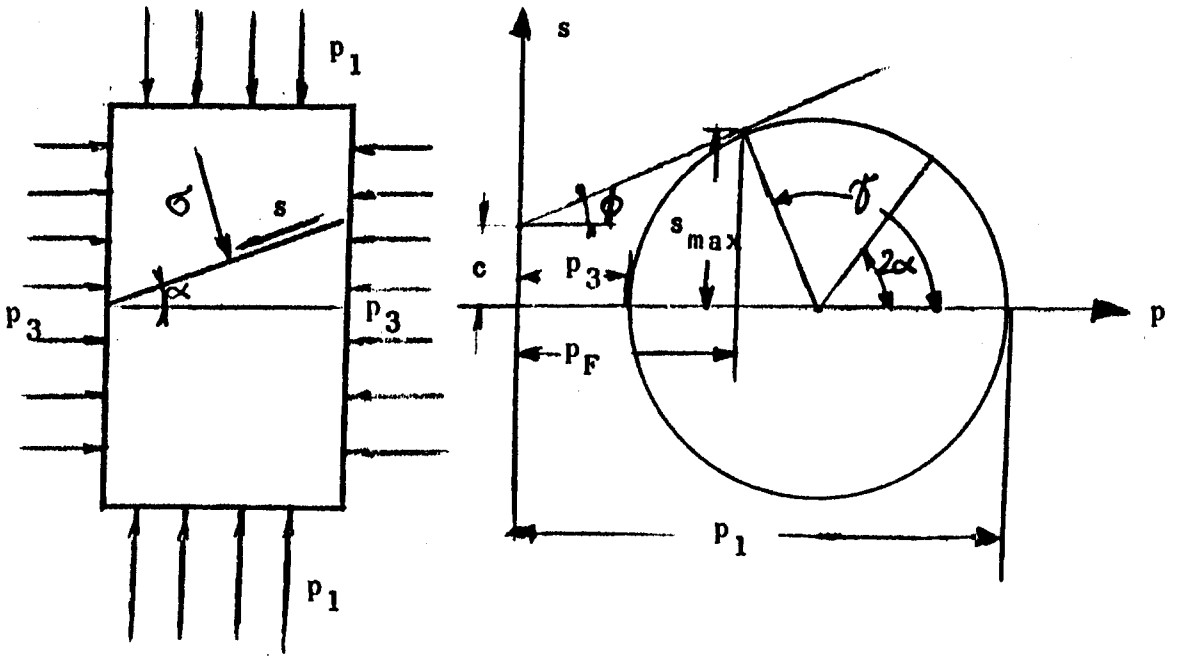

Figure 12.

When failure occurs the shear stress reaches the shear strength in the failure plane, according to Coulomb's criterion. Thus, s_{max} has to satisfy the equation of Mohr's circle and that of Coulomb's straight line (Equation 37). Thus,

$$s_{max} = \frac{p_1 - p_3}{2} \sin \gamma = c + p \tan \phi \quad \ldots\ldots (38)$$

(Here p_1 and p_3 are the stresses applied at failure).

Since $\gamma = \frac{\pi}{2} + \phi$

$$\frac{\gamma}{2} = \alpha_F = \frac{\pi}{4} + \frac{\phi}{2} \quad \text{for the failure plane.}$$

Thus, ϕ can be evaluated when α_F is known.

From Equations 38 and 39:

$$\frac{p_1 - p_3}{2} \sin \left(\frac{\pi}{2} + \phi\right) = c + p_F \tan \phi \quad \ldots (40)$$

or

$$\frac{p_1 - p_3}{2} \cos \phi = c + p_F \tan \phi$$

and

$$c = \frac{p_1 - p_3}{2} \cos \phi - p \tan \phi \quad \ldots\ldots\ldots (41)$$

The value of p, however, is still unknown.

From Figure 12:

$$p_F = p_3 + \frac{p_1 - p_3}{2} + \frac{p_1 - p_3}{2} \cos\gamma$$

$$p_F = \tfrac{1}{2}(p_1 + p_3) + \tfrac{1}{2}(p_1 - p_3) \cos(\frac{\pi}{2} + \phi)$$

Thus,

$$p_F = \tfrac{1}{2}(p_1 + p_3) - \tfrac{1}{2}(p_1 - p_3) \sin\phi \quad \ldots\ldots (42)$$

Since it is difficult to measure α_F, it is advisable to perform two or more triaxial tests with various p_3 values.

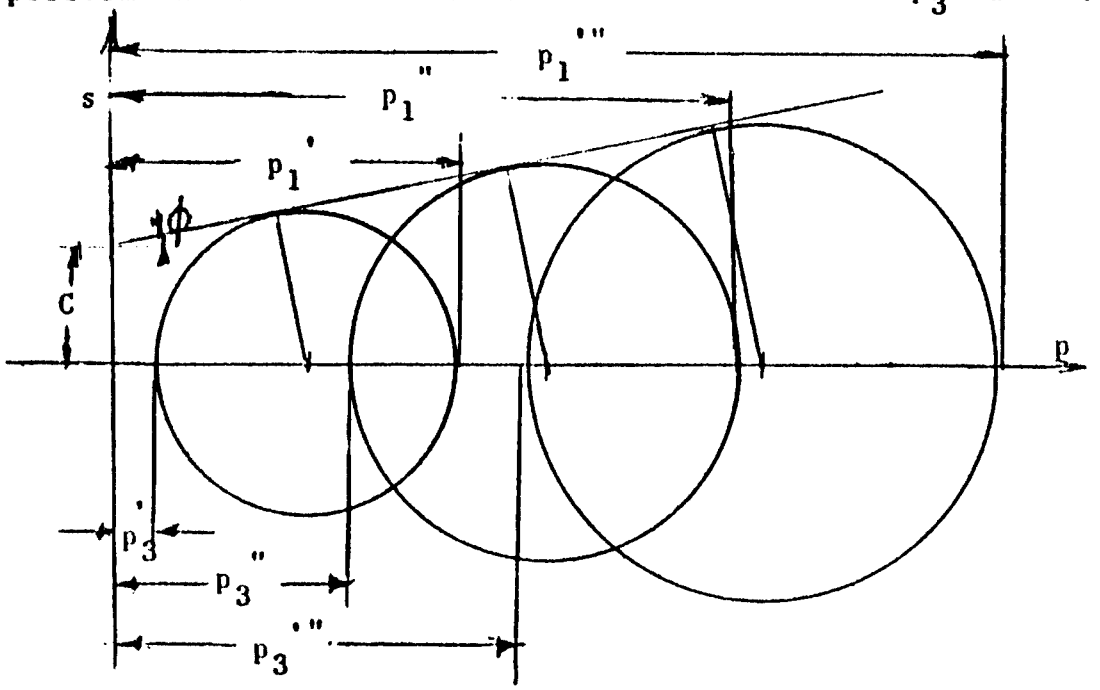

Fig. 13

Then, p, will vary at failure. By knowing p_3', p_1', p_3'', p_1'', etc., the envelope of the Mohr circles (which actually approximates a straight line) may be obtained. Its angle of

inclination is ϕ and its intercept with the s axis is c. Since a triaxial test is a slow procedure, it is not suitable to obtain a large number of soil values in a short time. Therefore, quicker procedures have been devised. Bekker proposed a shear apparatus in which a normal load and a torque is applied on an annulus which rests on the soil surface (17, 41). Thus, the average normal and shear stress acting in the horizontal plane directly under the ring ($s_{\theta av}$) can be recorded. The shear stress which is recorded at failure is considered equal to $s_{max.} = c + p \tan \phi$, where p is the normal pressure applied.

Actually, it is not evident that the failure occurs in the horizontal plane. Thus, the recorded value may be a shear stress value which acts in the horizontal plane while failure occurs and $s_{max.}$ may act in some other plane. Experimental evidence clearly shows, however, that the maximum torque per annulus area reading is a linear function of the normal pressure applied. The relationship may be expressed by means of an equation similar to Coulomb's.

$$s_{max.} = c_B + p \tan \phi_B \quad \ldots\ldots\ldots \quad (43).$$

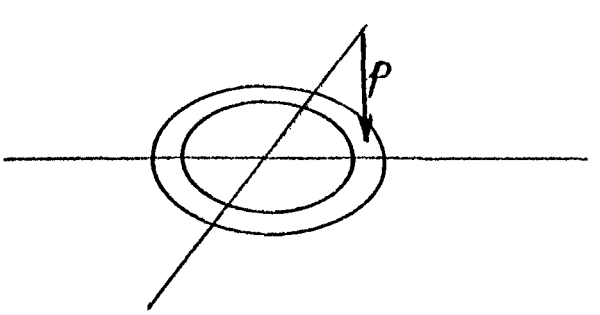

Figure 14.

Here index "B" stands for "Bekker's coefficient", as opposed to Coulomb's cohesion and friction angle. The relationship between c_B and c, as well as between ϕ and ϕ_B, is not clear as yet. Since c_B and ϕ_B is more suitable to describe vehicle operation in soft soils than c and ϕ, Land Locomotion Mechanics studies use the former sets of parameters. Thus, c_B and ϕ_B will be used and index "B" will be dropped henceforth.

An experimental shear stress-strain curve is of the shape shown in Figure 15 in most cases. Sometimes a hump and decay occurs as shown in Figure 16:

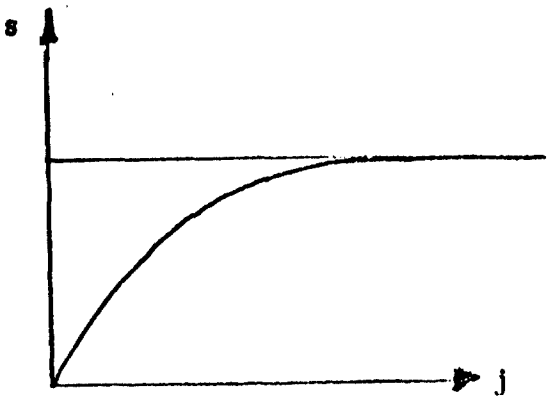

Figure 15.

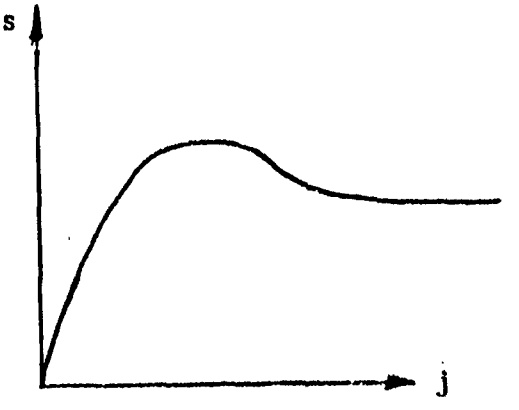

Figure 16.

Bekker introduced an empirical equation, similar to that derived for an overdamped one degree of freedom spring-mass system and proposed two additional soil values (K_1 and K_2) to replace the damping and the natural frequency of the undamped

system [5]. Weiss constructed a nomogram which enabled one to evaluate K_1 and K_2.[43]. Practice has shown, however, that the hump bears no practical importance because it occurs only at certain undisturbed clay soils which are not surface materials[44]. Furthermore, the effect of a hump may be neglected in the integration of shear stresses over a solid boundary because the deformations associated with the hump occur only under a relatively small part of the soil-vehicle interface surface. Experiments show that the hump decreases and finally disappears as p increases. When the curve is similar to that shown in Fig. 15, the following expression lends itself to replace Bekker's equation:

$$s = s_{max}(1 - e^{-j/K}) \quad \ldots\ldots\ldots \quad (44)$$

Equation 44, cannot be derived by a limit process from Bekker's equation unless some approximative assumptions are made.[45]. Similar relationships were arrived at by Nuttal (13), Soehne (29) and Weinblum (28).

The physical meaning of K can be seen in Fig. 17. Accordingly, K is the abscissa of the intersection of the

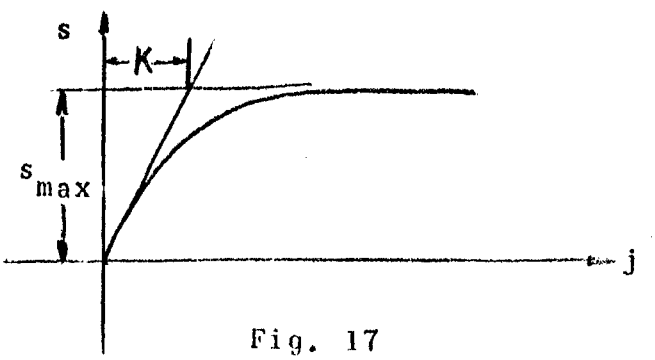

Fig. 17

curve ($s = s_{max}$) and the tangent drawn at the origin

$$s = \left[\left(\frac{ds}{dj}\right)_{j=o} j\right]$$

Since $$\left(\frac{ds}{dj}\right)_{j=o} = \frac{s_{max}}{K}$$

the equation $$\left(\frac{ds}{dj}\right)_{j=o} j = s_{max}$$

is satisfied when $K = j$. Thus, K is the abscissa of the point described above.

Therefore, one can obtain the numerical value of K by drawing the tangent at the origin and finding its intersect with the asymptote.

Reece suggested another method to evaluate the numerical value of K in his discussion of Paper No. 41 at the First International Conference on the Mechanics of Soil-Vehicle Systems. (Also see Ref. 45). He reasoned that if

$$\frac{s}{s_{max.}} = \left(1 - e^{-j/K}\right)$$

then $$\log\left(\frac{s}{s_{max.}} - 1\right) = -\frac{j}{K}$$

So the log of $\frac{s}{s_{max}} - 1$ is proportional to j. (The factor of proportionality being K). Therefore, if one plots $\left(\frac{s}{s_{max}} - 1\right)$ on a logarithmic axis and j on a linear scale, K will represent the slope of the straight line $j = \log\left(\frac{s}{s_{max}} - 1\right)$.

Equation 44 only approximates a true shear curve, hence one seldom obtains a continuous straight line when replotting the experimental shear curve on a semi-log paper. Therefore, the argument for Reece's method emphasizes that one is free to consider a larger portion of the curve than the initial one which is often not clearly definable.

Next, the question arises as to how K is influenced by the normal load (p), the dimensions of the Bevameter annulus and possibly some other factors. In other words, does K solely depend on the soil and its state? It is most likely that this is not so. A limited number of test results obtained at the Land Locomotion Laboratory seem to indicate that K is proportional to the circumference of the annulus. K also increases with the normal pressure, but it becomes constant when the normal pressure surpasses 3 - 4 psi.

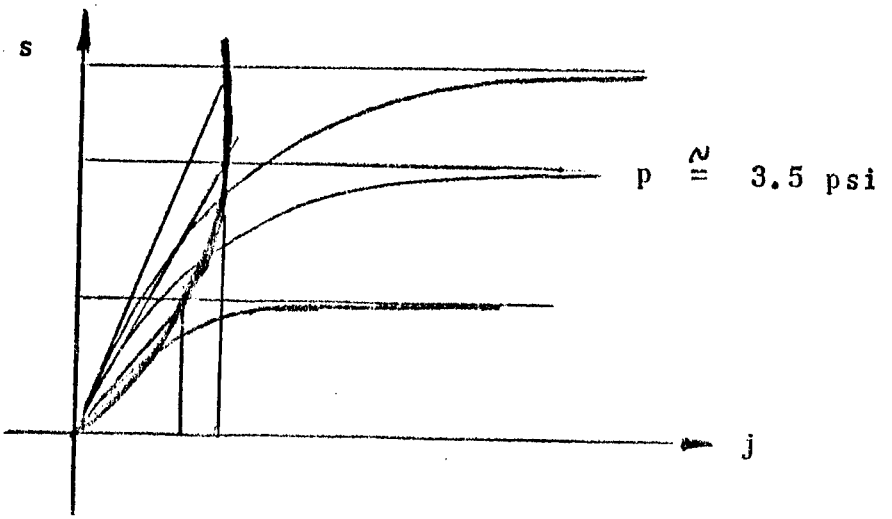

Fig. 18

J. Adams[45], investigated this problem in his Master's Thesis completed under the supervision of A. Reece. He found that K is proportional to $s_{max.}$. He recommended the following equation:

$$s = s_{max.}\left(1 - \bar{e}^{\frac{j}{K\, s_{max.}}}\right)$$

Here K refers to the tangent modulus measured at $s_{max.} = 1$ lb/in^2. In his experiments, shear tests were carried out by a shear block and not an annulus and the "semi-log" technique was used instead of the "tangent method" to evaluate K.

It is suggested that a broader investigation is required to elucidate the true nature of the various effects which influence K.

INTEGRATION OF SHEAR STRESSES

The term $$H = \int_{2\pi-\beta_o}^{2\pi} dT \cos\theta \qquad \text{(Equation 9-a)}$$

is analyzed in the following. Clearly:

$$dT = s\, b\, \frac{D}{2}\, d\theta \quad . \quad . \quad . \quad . \quad . \quad . \quad . \quad (45)$$

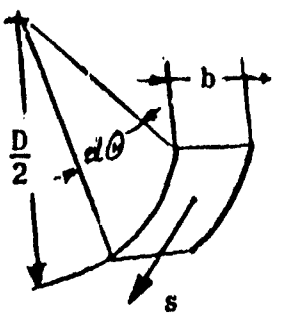

Figure 19.

or by Equation 44

$$dT = s_{max}(1 - e^{-j/K}) \frac{bD}{2} d\theta \quad \ldots\ldots(46)$$

From Equation 43:

$$dT = (c + p \tan \phi)(1 - e^{-j/K}) \frac{bD}{2} d\theta \quad \ldots\ldots(47)$$

Thus

$$H = \frac{bD}{2} \int_{2\pi - \beta_o}^{2\pi} (c + p \tan \phi)(1 - e^{-j/K}) \cos \theta \, d\theta \quad \ldots(48)$$

The next problem is to relate j and θ.

If one approximates the wheel as shown in Fig. 20, then the following assumptions may be made.

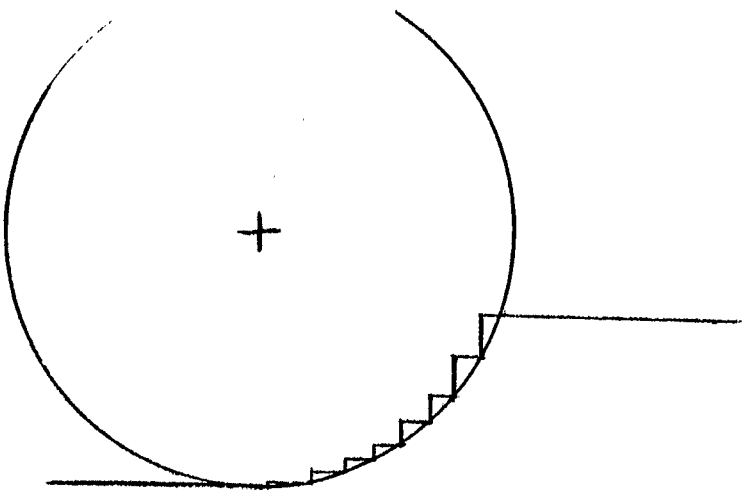

Fig. 20

The horizontal component of T is a function of the normal pressure prevailing at z and the horizontal component of the total deformation. The annulus sinks into the ground during

a shear test but only the horizontal deformation is recorded. The soil values obtained correspond to horizontal deformation components. Another question to be cleared with respect to this problem is the following. The normal pressure is varying from zero to p. The assumption that the shear stress created is the same as measured under p = constant may not be true.

According to Figure 21, the deformation at θ is

$$j_2 = \int_{2\pi - \beta_0}^{x_\theta} dx = \int_{2\pi - \beta_0}^{\Theta} \frac{dx}{d\theta}\, d\theta \quad \ldots . \quad (49)$$

From equation 14a:

$$\frac{dx}{d\theta} = \frac{D}{2} \left[(1 - i_0) - \cos \theta\right] \quad \ldots . \quad (50)$$

Thus,

$$j_2 = \frac{D}{2} \int_{2\pi - \beta_0}^{\theta} \left[(1 - i_0) - \cos \theta\right] d\theta \quad . . \quad (51)$$

When

$$2\pi - \beta_0 < \theta \leq 2\pi - \cos^{-1}(1 - i_0) - \quad \text{(Region 2).}$$

Hence

$$j_2 = \frac{D}{2} \left[(1 - i_0)(\theta - 2\pi + \beta_0) - \sin \theta - \sin \beta_0\right] . . (52)$$

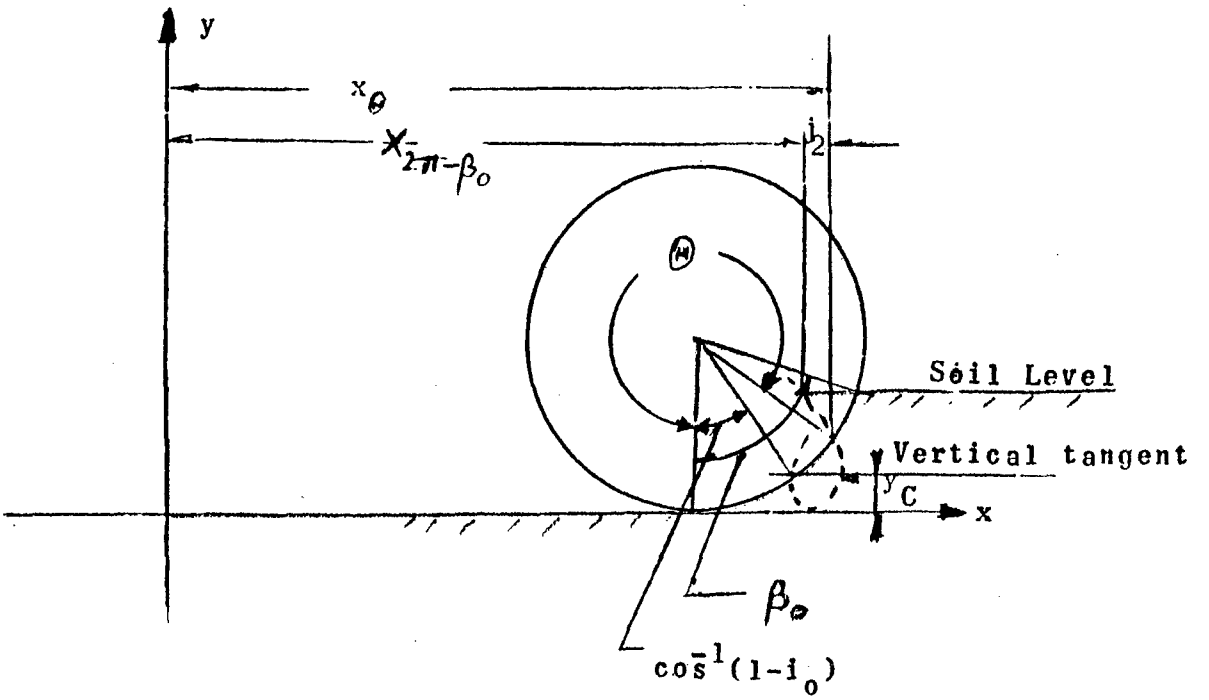

Figure 21.

As Θ becomes greater than $\cos^{-1}(i - i_o)$, Region 3, the direction of the deformation changes and a negative j will be generated (Figure 22). In order to maintain a negative exponent in Equation 40, j has to be obtained for:

$$2\pi - \beta_o \leq 2\pi - \cos^{-1}(1 - i_o) < \theta \leq 2\pi \text{ as shown below:}$$

$$j_1 = -\int_{2\pi - \cos^{-1}(1 - i_o)}^{\theta} \frac{dx}{d\theta}\, d\theta = \int_{\theta}^{2\pi - \cos^{-1}(1 - i_o)} \frac{dx}{d\theta}\, d\theta \quad . \quad . \quad . (53)$$

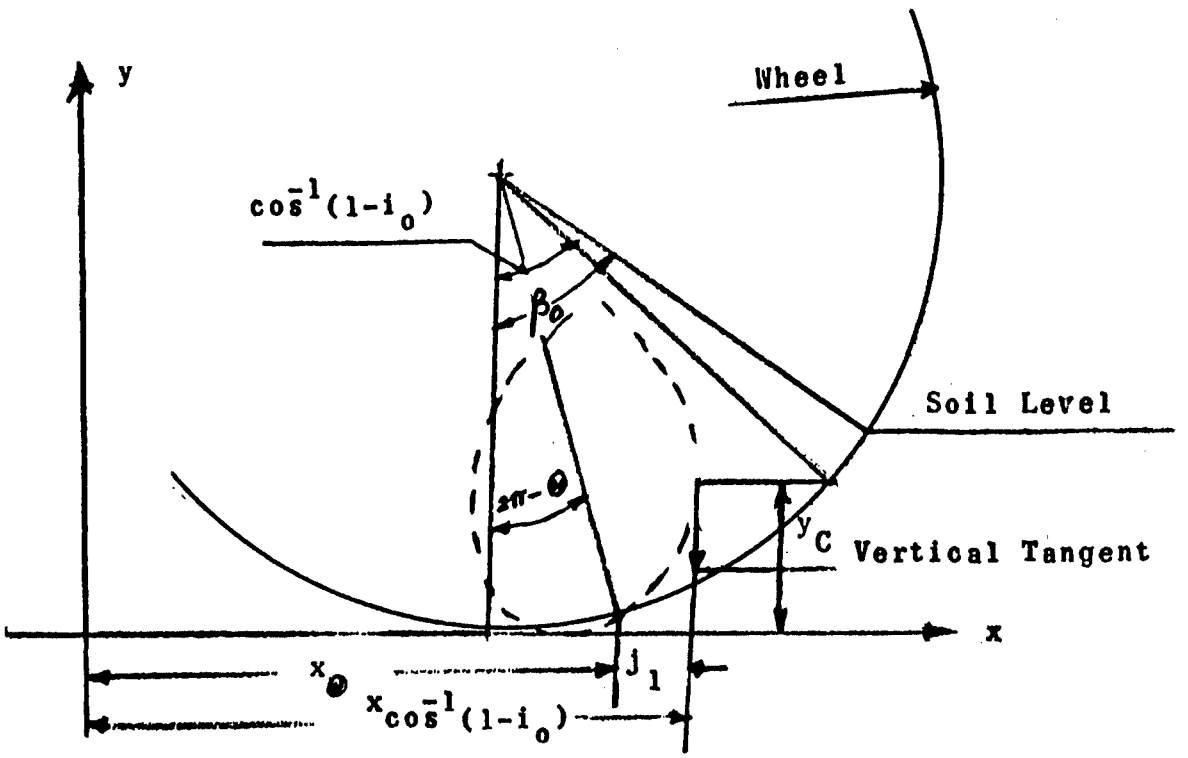

Fig. 22

or

$$j_1 = [(1 - i_o)(\theta_v - \theta) - \sin\theta_v + \sin\theta] \quad \ldots\ldots (54)$$

where $$\theta_v = 2\pi - \cos^{-1}(1 - i_o) \quad \ldots\ldots\ldots (55)$$

The sum of the shear stresses along the soil-wheel interface becomes: $$H = H_1 - H_2 \quad \ldots\ldots\ldots\ldots (56)$$

where

$$H_1 = \frac{bD}{2} \int_{\theta_v}^{2\pi} (c + p \tan \phi)(1 - \bar{e}^{j_1/K}) \, d\theta \quad \ldots (57)$$

$$H_2 = \frac{bD}{2} \int_{2\pi - \beta_o}^{\theta_v} (c + p \tan \phi)(1 - \bar{e}^{j_2/K}) \, d\theta \quad \ldots (58)$$

Equations 56, 57, 58, 54 and 52, allow one to evaluate the traction of a wheel when the sinkage is larger than y_c. In other words, when the sinkage is deep enough to cause soil-wheel contact along that region of the wheel perimeter (Region 2) whose points move forward and downward. Using our notations, Equation 56 is to be used when $\beta_o > 2\pi - \theta_v$. When $\beta_o < 2\pi - \theta_v$ only Region 3 has to be considered.

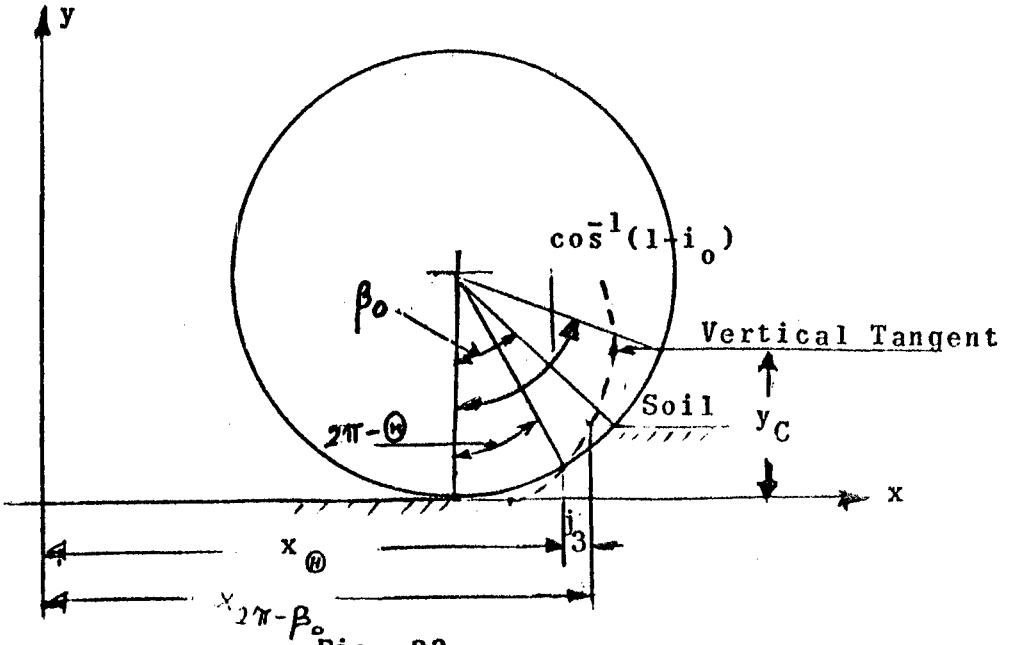

Fig. 23

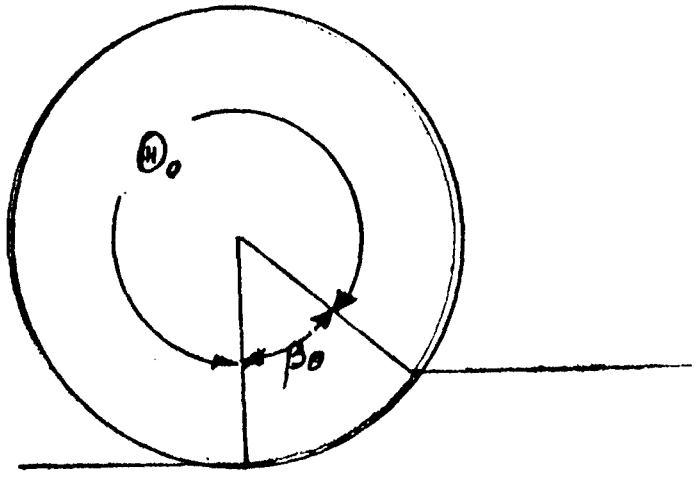

Figure 24.

Here, Figure 23:

$$j_3 = -\int_{2\pi-\beta_o}^{\theta} \frac{dx}{d\theta}\, d\theta$$

where

$$\theta_v \leq 2\pi - \beta_o \leq \theta \leq 2\pi$$

$$j_3 = \int_{\theta}^{2\pi-\beta_o} \frac{dx}{d\theta}\, d\theta = \frac{D}{2}\,[(1 - i_o)(2\pi - \beta_o) - \theta$$

$$+ \sin\beta + \sin\theta] \qquad \ldots\ldots\ldots\ldots (59)$$

Thus $$H = \frac{bD}{2} \int_{2\pi-\beta_o}^{2\pi} (c + p \tan \phi)(1 - \bar{e}^{\frac{j_3}{-K}}) \, d\theta \quad . \; . \; . \; (60)$$

Equation 60, yields the tractive force when (See Equation 3):

$$\cos^{-1}(1 - i_o) \geq \beta_o = \cos^{-1}(1 - \frac{2z_o}{D})$$

Before Equation 56 or Equation 60 can be programmed for an electronic computer, p has to be expressed as a function of θ.

Equation 4, yields the expression desired:

$$p = (\frac{k_c}{b} + k_\phi) \left[(\cos \theta - \cos \theta_o) \frac{D}{2}\right]^n \quad . \; . \; (4)$$

The foregoing method may be summed as follows:

1. Find z_o (Equation 7)
2. Find β_o (Equation 3)
3. Find $\theta_v = \cos^{-1}(1 - i_o)$
4. If $\beta_o > 2\pi - \theta_v$ (Use equations 4, 53, 54, 57, 58 and 56 to find H)
5. If $\beta_o \leq 2\pi - \theta_v$ (Use Equations 4, 59 and 60)
6. Subtract R (Equation 6) from H.

The following input data are necessary to perform the calculations: k_c, k_ϕ, n , c, ϕ, K, D, b, W, i_o. The variable is Θ naturally.

REFERENCES

1. Bernstein, R., "Probleme zur Experimentellen Motoroflug Motorwagen, 1913.

2. Goryachkin, V. D., (collective work), "Tedria i Prosivodstuvo Sielskohoziayniti Mashin", Moscow, 1936.

3. Garbari, F., "Resistenza al Movimento Dei Veicoli a Route so Terreno Cedevole", Ata, Rendiz Congr. 9-11.

4. Bekker, M. G., "A Proposed System of Physical and Geometric Terrain Values for the Determination of Vehicle Performance and Soil Trafficability", Interservice Vehicle Mobility Symposium, Office of Ordnance Research, Duke University and Stevens Institute of Technology. Published by Land Locomotion Research Branch, OTAC, Detroit, 1955.

5. Bekker, M. G., "Theory of Land Locomotion", (Chapter VI), University of Michigan Press, Ann Arbor, Michigan, 1956.

6. Vincent, E. T., "Pressure Distribution On and Flow of Sand Past a Rigid Wheel", First International Conference on the Mechanics of Soil-Vehicle Systems, Turin, 1961.

7. Hegedus, E., "A Preliminary Analysis of the Force System Acting on a Rigid Wheel", Report No. 74, Land Locomotion Laboratory, OTAC, Detroit Arsenal, Centerline, Mich., 1962.

8. Tanaka, T., "The Statistical Analysis and Experiment on the Force to the Tractor Wheel", Paper No. 18, First International Conference on Research and Engineering Mechanics of Soil-Vehicle Systems, Turin, 1961

9. Phillips, J., "A Discussion on Slip and Rolling Resistance", Paper No. 54, First International Conference on the Mechanics of Soil-Vehicle Systems, Turin, 1961.

10. Uffelmann, F. L., "The Performance of Rigid Cylindrical Wheels on Clay Soil", Paper No. 7, First International Conference on Research and Engineering Mechanics of Soil-Vehicle Systems, Turin, 1961.

11. Schuring, D., "On the Mechanics of Rigid Wheels on Soft Soil", (in German) VDI, June 1961.

12. Hicks, H. H., "A Similitude Study of the Drag and Sinkage of Wheels Using a System of Soil Values Related to Locomotion", Paper No. 38, First International Conference on the Mechanics of Soil-Vehicle Systems, Turin, 1961.

13. Nuttal, C. J. and McGowan, R. P., "Scale Models of Vehicles in Soils and Snows", Paper No. 39, First International Conference on the Mechanics of Soil-Vehicle Systems, Turin, 1961.

14. Andreev, A. A., "Analytical Treatment of Certain Problems in the Kinematics of Wheels of Agricultural Machines", (in Russian), Sborn. Trud. Po Zemledel'chesk, Mekh. 2 3-12, 1954 USSR.

15. Omelyanov, A. E., "O Primenii Pneumatichenih Koles", Selhozmashina, No. 5, 1948.

16. Ageykin, Y. S., "Opredechenie Deformatsii Parametrov Kontakta Shiny s Myagkim Gruntom", Autom. Trakt. Prom 1959 (5).

17. "A Soil Value System for Land Locomotion Mechanics", Report No. 5, Land Locomotion Laboratory, OTAC, Detroit Arsenal, Centerline, Mich., 1958.

18. Janosi, Z., "Soil Values in Land Locomotion", Journal of Agricultural Engineering Research, Vol. 5, No. 1, 1960.

19. Bekker, M. G. and Janosi, Z., "Analysis of Towed Pneumatic Tires Moving on Soft Ground", Report No. 62, Land Locomotion Laboratory, OTAC, Detroit Arsenal, Centerline, Michigan.

20. Bekker, M. G., "Off-the-Road Locomotion", University of Michigan Press, Ann Arbor, Michigan, 1960.

21. Reed, I. F., "Pressure Patterns for Conventional and Radial Ply Tires", Presented at the meeting of the ASAE Committee on Tractive and Transport Efficiency at the National Tillage Laboratory, Auburn, Alabama, 1960.

22. Thompson, A. B. and Smith, M. E., "Stresses Under Moving Vehicles". Technical Report No. 3-5445, Report 2, U. S. Army Engineer, Waterways Experiment Station, Corps of Engineers, Vicksburg, Mississippi, 1960.

23. Soehne, W., "Druckverteilung im Boden und Bodenverformung Unter Schlepperreifen", Grundlagen der Landtechnik, Vol. 5, 1953.

24. Vandenberg, G. E., Cooper, A. W., Erickson, A. E., "Soil Pressure Distribution Under Tractor and Implement Traffic", Agricultural Engineering, Vol. 38, No. 12, December 1957.

25. Kerr, R. C., "A Design Guide for the Application of Pneumatic Tires to Vehicles Intended for Off-Road Service", Arabian American Oil Company, 1955.

26. Chapoux, E., "Pneumatic Pour Vehicles Sahariens", Engineur de l'Automobil, Vol. XXXII, No. II, 1959.

27. Weinblum, M. and Orlowski, S., "Factors Affecting Wheeled Tractor Traction on Sandy Loose Soils", Paper No. 51, First International Conference on the Mechanics of Soil-Vehicle Systems, Turin, 1961.

28. Sohne, W. and Sonnen, F. I., "Rolling Resistance and Drawbar Pull Measurements of Wheeled Tractors as well as an Investigation of Soil Value Systems", (in German), Paper No. 32, First International Conference on the Mechanics of Soil-Vehicle Systems, Turin, 1961.

29. Turnbull, W. J. and Freitag, D. R., "Influence on Soil Factors and Tire Geometry on the Performance of Pneumatic Tires in Sand", Paper No. 31, First International Conference on the Mechanics of Soil-Vehicle Systems, Turin, 1961.

30. Mazza, C. and Amici, "Essais sur Pneus Pour Tracteurs Influence de la Structure de la Carcassee", R. G. C., Vol. 36, No. 10, 1959.

31. Vandenberg, G. E. and Reed, I. F., "Tractive Performance of Radial Ply and Conventional Tractor Tires", Paper No. 61-608, Winter Meeting of ASAE Chicago, December 1961.

32. Richey, C. B., "Techniques for Field Test Comparison of Tractor Tire Efficiency", Presented at the meeting of the ASAE Committee on Tractive and Transport Efficiency at the National Tillage Laboratory, Auburn, Alabama, 1960.

33. Hegedus, E., "Evaluation of Condual Tire Model", Report No. 60, Land Locomotion Laboratory, OTAC, Detroit Arsenal, Centerline, Michigan, 1960.

34. Hadekel, R., "The Mechanical Characteristics of Pneumatic Tires", Issured by T.P.A. 3, Technical Information Bureau for Chief Scientists, Ministry of Supply, England, 1944.

35. Trabbic, G. W., "The Effect of Drawbar Load and Tire Inflation on Soil-Tire Interface Pressure", Master of Science Thesis, Michigan State University, Dept. of Agricultural Engineering, 1959.

36. Ehrlich, I. R., "Wheel Sinkage in Soils", Ph.D. Thesis, University of Michigan, 1960.

37. Hegedus, E., "A Simplified Method for the Determination of the Bulldozing Resistance", Report No. 61, Land Locomotion Laboratory, OTAC, Detroit Arsenal, Centerline, Mich., 1960.

38. Janosi, Z., "An Analysis of Pneumatic Tire Performance on Deformable Soils", Paper No. 42, First International Conference on the Mechanics of Soil-Vehicle Systems, Turin, 1961.

39. Coulomb, C. A., "Essai sur une Application de Maximis et Minimis a Quelques Problemes de Statique Relatifs a L'architecture, Mem. Div. Sav. Academie des Sciences, Paris, Vol. 7, 1773, p. 343.

40. Terzaghy, K., "Theoretical Soil Mechanics", John Wiley & Sons, New York.

41. "A Soil Value System for Land Locomotion Mechanics", Research Report No. 5, Land Locomotion Laboratory, OTAC, U. S. Army, Detroit Arsenal, Centerline, Michigan, 1958.

42. Weiss, J. S., "Preliminary Study of Snow Values Related to Vehicle Performance", Report No. 2, Land Locomotion Laboratory, OTAC, Detroit Arsenal, 1956.

43. Goodman, L. J., "The Influence of Remolding or Disturbance to Clay Soils on Mobility Problems", Syracuse University Research Institute College of Engineering, 1961.

44. Adams, J., "An Analysis of Tracklayer Performance", MS Thesis, Agricultural Engineering Department, University of Durham, 1961.

TECHNICAL REPORT DISTRIBUTION LIST

DATE: JUNE 1963

Report No. 8091
LL No. 84

PROJECT TITLE: PERFORMANCE ANALYSIS OF A DRIVEN NON-DEFLECTING TIRE IN SOIL.

Address	Copies
Director, Research and Engineering Directorate (SMOTA-R)	1
Components Research and Development Laboratories ATTN: Administrative Branch (SMOTA-RCA)	2
Components Research and Development Laboratories ATTN: Materials Laboratory (SMOTA-RCM)	1
Systems Requirements and Concept Division	
ATTN: Systems Simulations Branch (SMOTA-RRC)	1
ATTN: Systems Concept Branch (SMOTA-RRD)	1
ATTN: Economic Engineering Study Branch (SMOTA-RRE)	1
ATTN: Systems Requirements Branch (SMOTA-RRF)	1
ATTN: Foreign Technology Section (SMOTA-RTS.2)	1
ATTN: Technical Information Section (SMOTA-RTS)	2
Commanding General U. S. Army Mobility Command	
ATTN: AMSMO-RR	1
ATTN: AMSMO-RDC	1
ATTN: AMSMO-RDO Warren, Michigan 48090	1
USACDC Liaison Office (SMOTA-LCDC)	2
Sheridan Project Office (AMCPM-SH-D)	1
U. S. Naval Civil Engineering Research and Engineering Laboratory Construction Battalion Center Port Hueneme, California	1
Commanding Officer Yuma Proving Ground Yuma, Arizona 85364	1
Harry Diamond Laboratories Technical Reports Group Washington, D. C. 20025	1

Address	No. of Copies
Defense Documentation Center Cameron Station ATTN: TIPCA Alexandria, Virginia 22314	10
Commanding General Aberdeen Proving Ground ATTN: Technical Library Maryland 21005	2
Commanding General Hq, U. S. Army Materiel Command ATTN: AMCOR (TW)	1
ATTN: AMCOR (TB) Department of the Army Washington, D. C. 20025	1
Land Locomotion Laboratory	2
Propulsion Systems Laboratory	5
Fire Power Laboratory	1
Track and Suspension Laboratory	6
Commanding General U. S. Army Mobility Command ATTN: AMCPM-M60 Warren, Michigan 48090	3
Commanding General Headquarters USARAL APO 949 ATTN: ARAOD Seattle, Washington	2
Commanding General U. S. Army Aviation School Office of the Librarian ATTN: AASPI-L Fort Rucker, Alabama	1
Plans Officer (Psychologist) PP&A Div, G3, Hqs, USACDCEC Fort Ord, California, 93941	1
Commanding General Hq, U. S. Army Materiel Command Research Division ATTN: Research and Development Directorate Washington, D. C. 20025	1

Address	No. of Copies
Commandant Ordnance School Aberdeen Proving Ground, Md.	1
British Joint Service Mission Ministry of Supply P. O. Box 680 Benjamin Franklin Station ATTN: Reports Officer Washington, D. C.	2
Canadian Army Staff 2450 Massachusetts Avenue Washington, D. C.	4
British Joint Service Mission Ministry of Supply Staff 1800 K Street, N. W. Washington, D. C.	6
Director Waterways Experiment Station Vicksburg, Mississippi	3
Unit X Documents Expediting Project Library of Congress Washington, D. C. Stop 303	4
Exchange and Gift Division Library of Congress Washington, D. C. 20025.	1
Headquarters Ordnance Weapons Command Research & Development Division Rock Island, Illinois Attn: ORDOW-TB.	2
Army Tank-Automotive Center Canadian Liaison Office, SMOTA-LCAN.	4
United States Navy Industrial College of the Armed Forces Washington, D. C. Attn: Vice Deputy Commandant	10
Continental Army Command Fort Monroe, Virginia	1

Address	No. of Copies
Dept. of National Defense Dr. N. W. Morton Scientific Advisor Chief of General Staff Army Headquarters Ottawa, Ontario, Canada	1
Commanding Officer Office of Ordnance Research Box CM, Duke Station Durham, North Carolina	3
Chief Office of Naval Research Washington, D. C.	1
Superintendent U. S. Military Academy West Point, New York Attn: Prof. of Ordnance	1
Superintendent U. S. Naval Academy Anapolis, Md.	1
Chief, Research Office Mechanical Engineering Division Quartermaster Research & Engineering Command Natick, Massachusetts	1
Mr. M. Bahn Department 6101 Chrysler Defense Engineering Box 1316 Detroit 31, Michigan	1

AD _____ ACCESSION NO. _____

U.S.Army Tank-Automotive Center, Land Locomotion Laboratory, Detroit Arsenal, Center Line, Michigan.

PERFORMANCE ANALYSIS OF A DRIVEN NON-DEFLECTING TIRE IN SOIL, by Zoltan J. Janosi.

Report No. 8091 pp-50 June 1963
Project No. 5016.11.84400 Unclassified

This report presents the first semi-empirical solution suggested to describe the traction versus slip relationship for rigid wheels.

The kinematics of a slipping wheel are analyzed and the results are used to express the shear deformation as a function of slip which in turn is utilized in a new shear stress-strain relationship. The shear stresses are expressed at every point of the tire-soil interface surface and integrated to obtain the traction.

Other established information is also briefly discussed, in order to complete the description of the state-of-the-art.

-Unclassified-

Land Locomotion Laboratory

AD _____ ACCESSION NO. _____

U.S.Army Tank-Automotive Center, Land Locomotion Laboratory, Detroit Arsenal, Center Line, Michigan.

PERFORMANCE ANALYSIS OF A DRIVEN NON-DEFLECTING TIRE IN SOIL, by Zoltan J. Janosi.

Report No. 8091 pp-50 June 1963
Project No. 5016.11.84400 Unclassified

This report presents the first semi-empirical solution suggested to describe the traction versus slip relationship for rigid wheels.

The kinematics of a slipping wheel are analyzed and the results are used to express the shear deformation as a function of slip which in turn is utilized in a new shear stress-strain relationship. The shear stresses are expressed at every point of the tire-soil interface surface and integrated to obtain the traction.

Other established information is also briefly discussed, in order to complete the description of the state-of-the-art.

-Unclassified-

Land Locomotion Laboratory

AD _____ ACCESSION NO. _____

U.S.Army Tank-Automotive Center, Land Locomotion Laboratory, Detroit Arsenal, Center Line, Michigan.

PERFORMANCE ANALYSIS OF A DRIVEN NON-DEFLECTING TIRE IN SOIL, by Zoltan J. Janosi.

Report No. 8091 pp-50 June 1963
Project No. 5016.11.84400 Unclassified

This report presents the first semi-empirical solution suggested to describe the traction versus slip relationship for rigid wheels.

The kinematics of a slipping wheel are analyzed and the results are used to express the shear deformation as a function of slip which in turn is utilized in a new shear stress-strain relationship. The shear stresses are expressed at every point of the tire-soil interface surface and integrated to obtain the traction.

Other established information is also briefly discussed, in order to complete the description of the state-of-the-art.

-Unclassified-

Land Locomotion Laboratory

AD _____ ACCESSION NO. _____

U.S.Army Tank-Automotive Center, Land Locomotion Laboratory, Detroit Arsenal, Center Line, Michigan.

PERFORMANCE ANALYSIS OF A DRIVEN NON-DEFLECTING TIRE IN SOIL, by Zoltan J. Janosi.

Report No. 8091 pp-50 June 1963
Project No. 5016.11.84400 Unclassified

This report presents the first semi-empirical solution suggested to describe the traction versus slip relationship for rigid wheels.

The kinematics of a slipping wheel are analyzed and the results are used to express the shear deformation as a function of slip which in turn is utilized in a new shear stress-strain relationship. The shear stresses are expressed at every point of the tire-soil interface surface and integrated to obtain the traction.

Other established information is also briefly discussed, in order to complete the description of the state-of-the-art.

-Unclassified-

Land Locomotion Laboratory